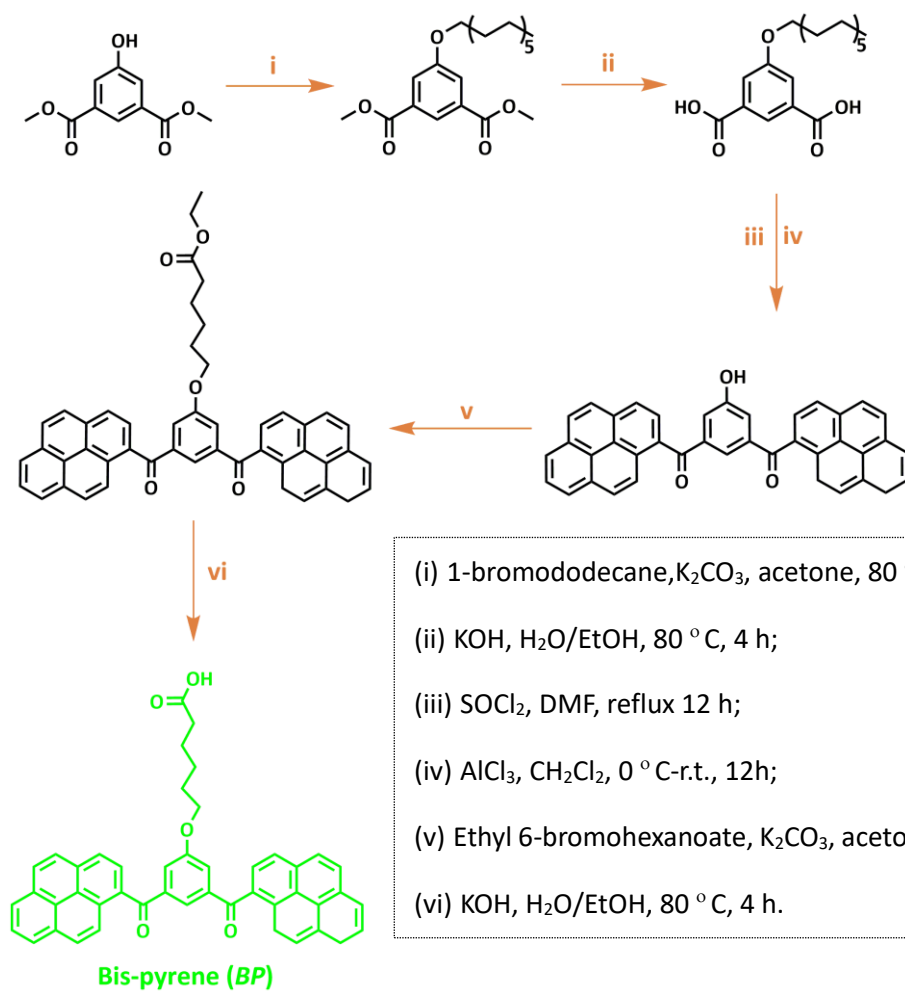


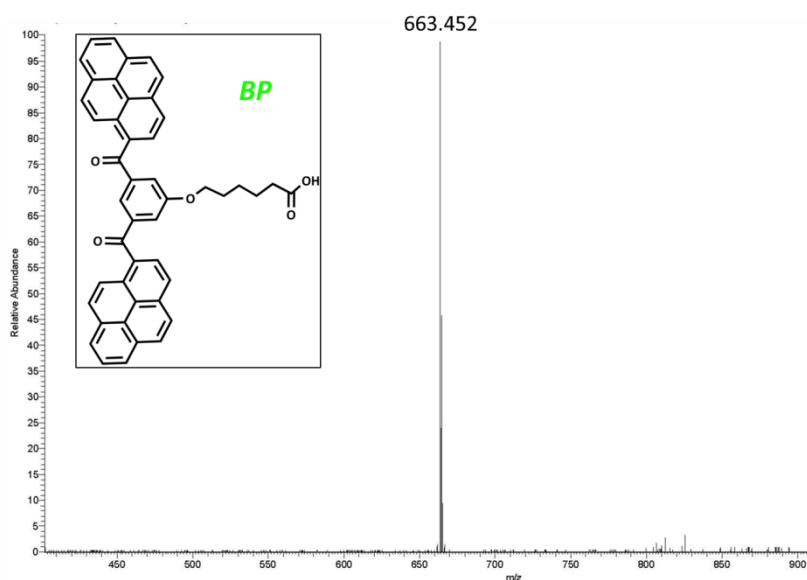
SUPPLEMENTARY INFORMATION

Transformable peptide nanoparticles arrest HER2 signalling and cause cancer cell death *in vivo*

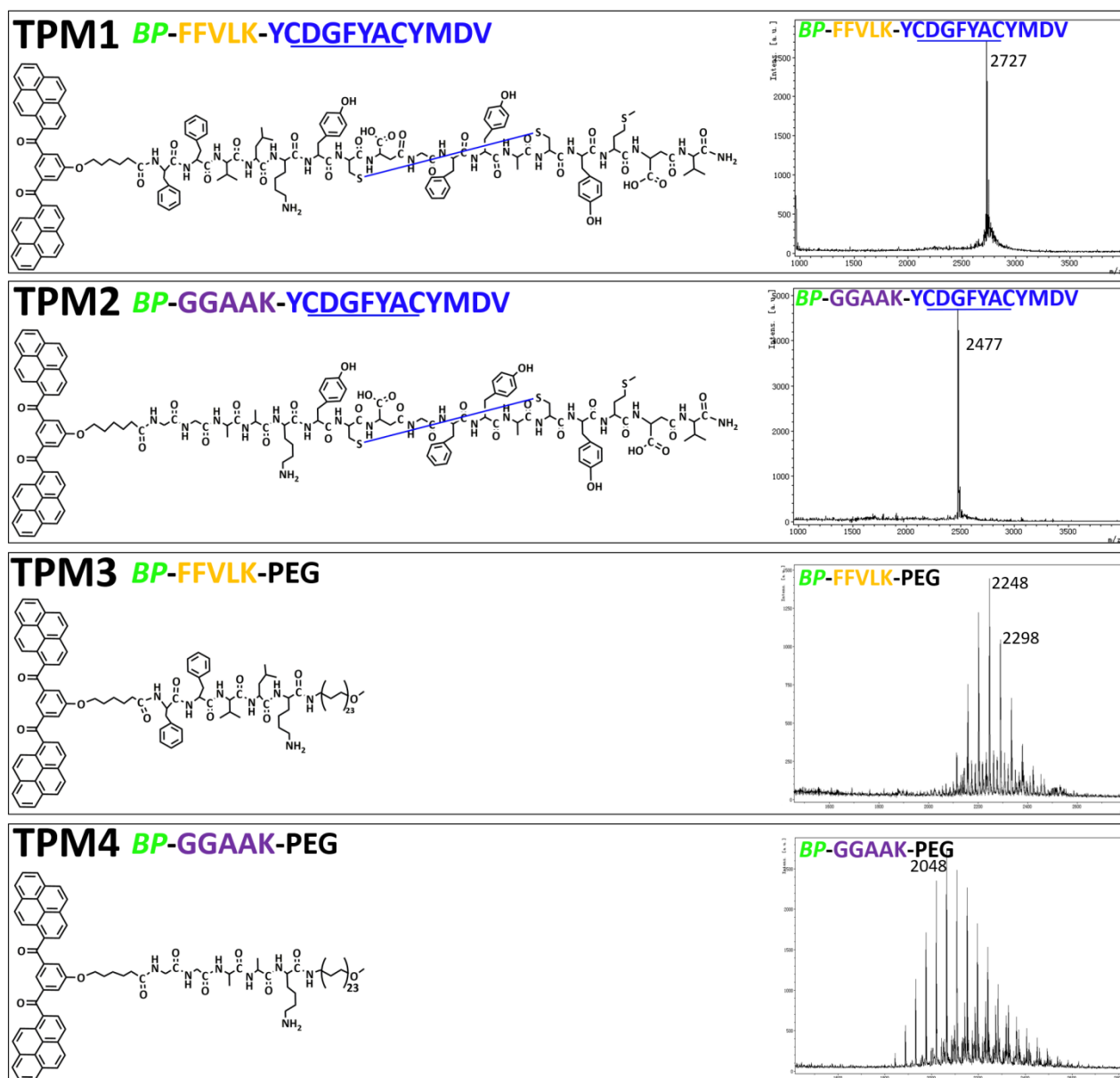
Lu Zhang¹, Di Jing¹, Nian Jiang^{2,4}, Tatu Rojalín¹, Christopher Michael Baehr¹, Dalin Zhang¹, Wenwu Xiao¹, Yi Wu¹, Zhaoqing Cong¹, Jian Jian Li², Yuanpei Li¹, Lei Wang^{3*} and Kit S Lam^{1,5*}



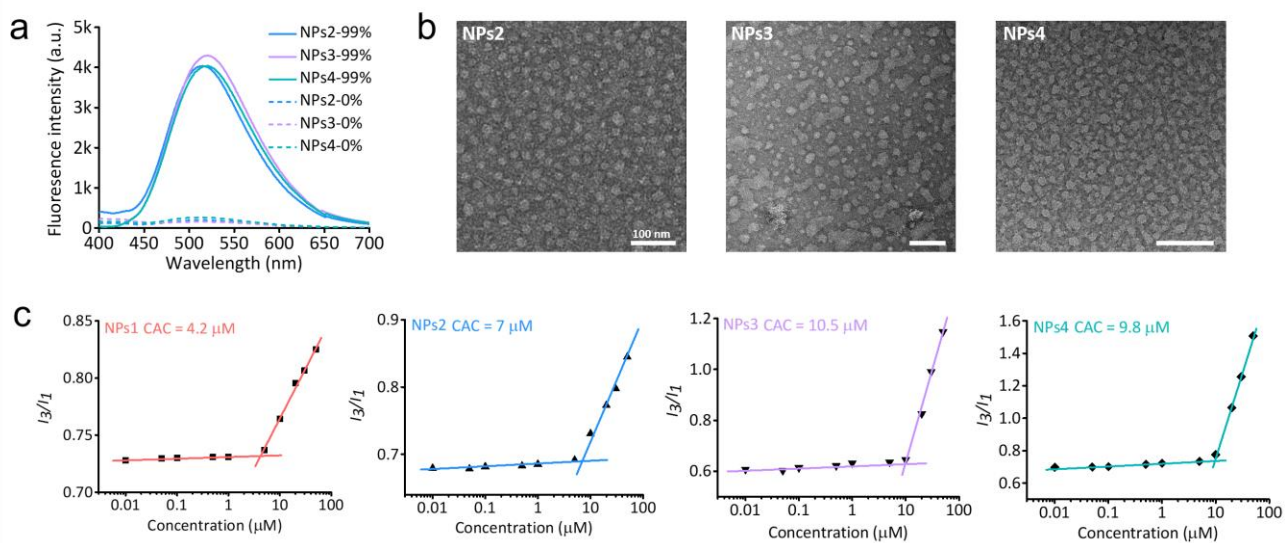
- (i) 1-bromododecane, K_2CO_3 , acetone, $80^\circ C$, 24 h;
(ii) KOH, $H_2O/EtOH$, $80^\circ C$, 4 h;
(iii) $SOCl_2$, DMF, reflux 12 h;
(iv) $AlCl_3$, CH_2Cl_2 , $0^\circ C$ -r.t., 12h;
(v) Ethyl 6-bromohexanoate, K_2CO_3 , acetone, $80^\circ C$, 24 h;
(vi) KOH, $H_2O/EtOH$, $80^\circ C$, 4 h.



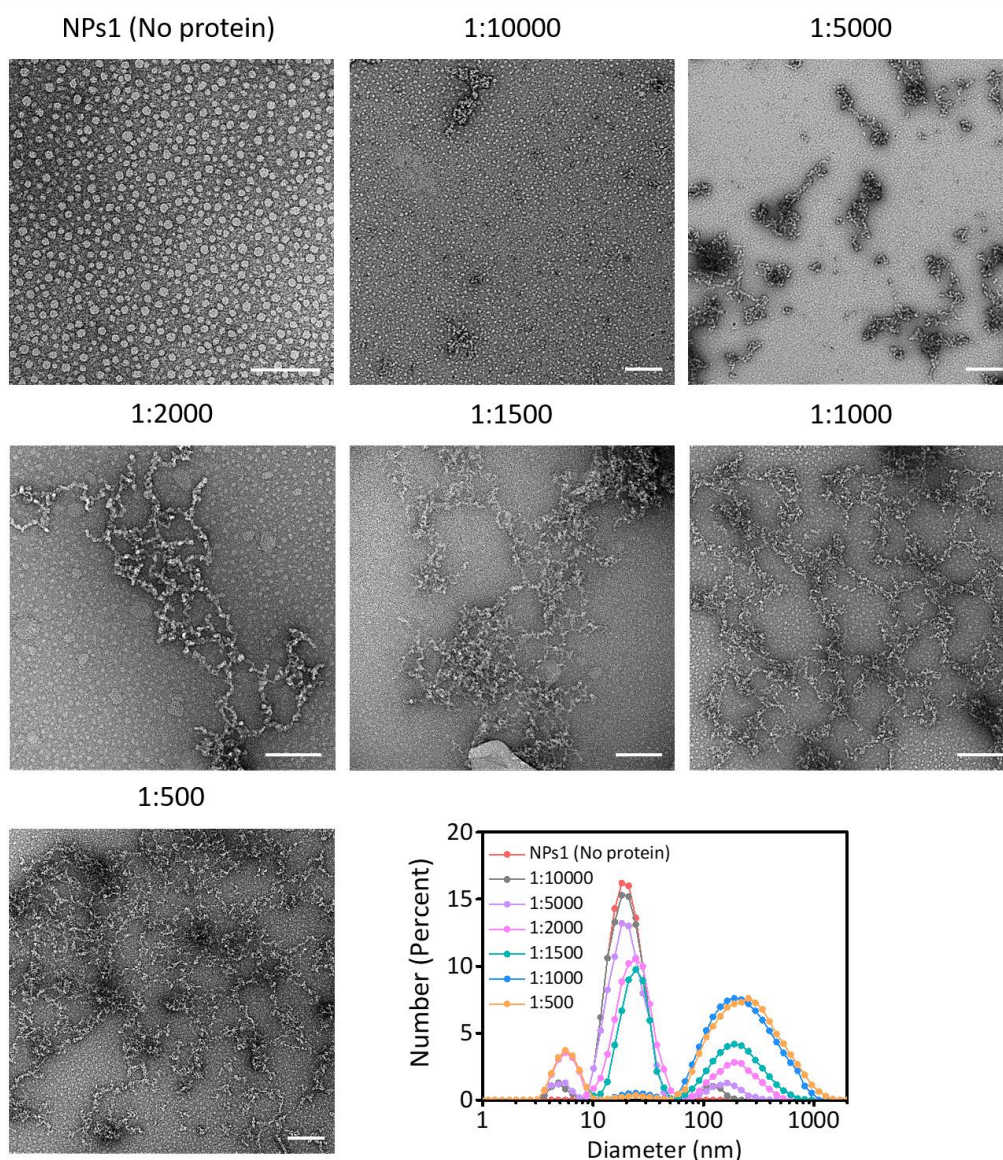
Supplementary Fig. 1. Synthetic approach of bis-pyrene (BP) molecule *via* multi steps chemical reactions and mass spectra *via* ESI of BP molecule.



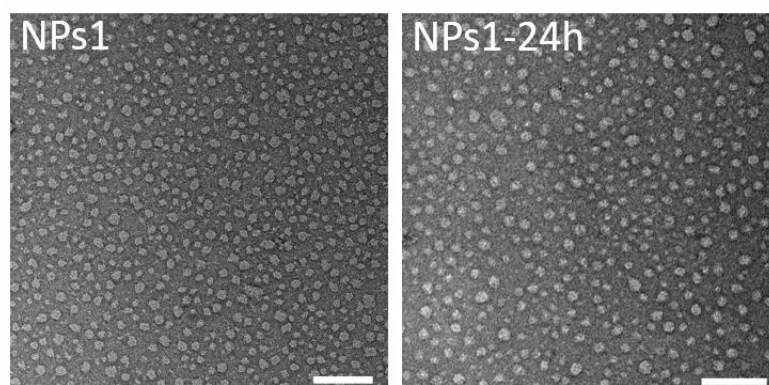
Supplementary Fig. 2. Chemical structure and mass spectra *via* MALDI-TOF of transformable peptide monomer (TPM) 1 *BP-FFVLK-YCDGFYACYMDV*, 2 *BP-GGAAK-YCDGFYACYMDV*, 3 *BP-FFVLK-PEG*, 4 *BP-GGAAK-PEG*. Experiments were repeated three times.



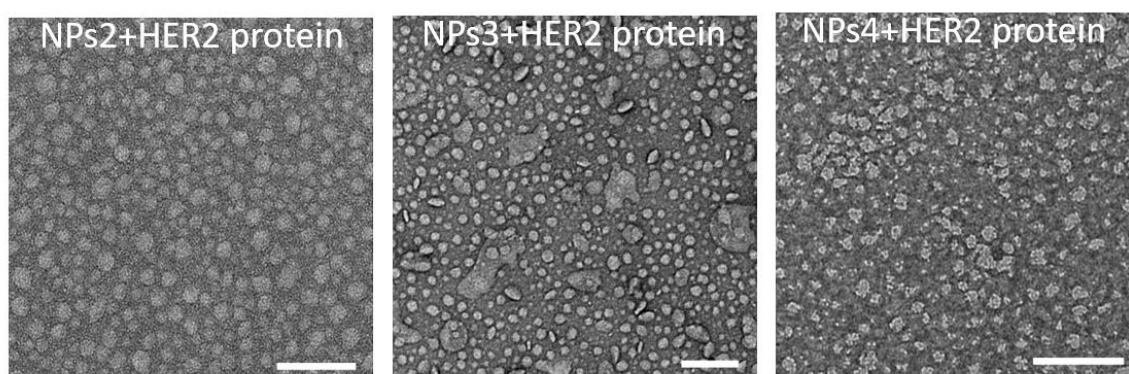
Supplementary Fig. 3. a, Changes in fluorescence signal of NPs2-4 solution with different H₂O:DMSO ratio (0:100 and 99:1). *Ex* = 380 nm. Experiments were repeated three times. **b**, TEM images of NPs2-4 at the H₂O and DMSO ratio of 99:1. NPs2-4 concentration was kept constant at 20 μM . Experiments were repeated three times. **c**, The critical aggregation concentration (CAC) of NPs1-4 was measured by using pyrene as a probe. Experiments were repeated three times.



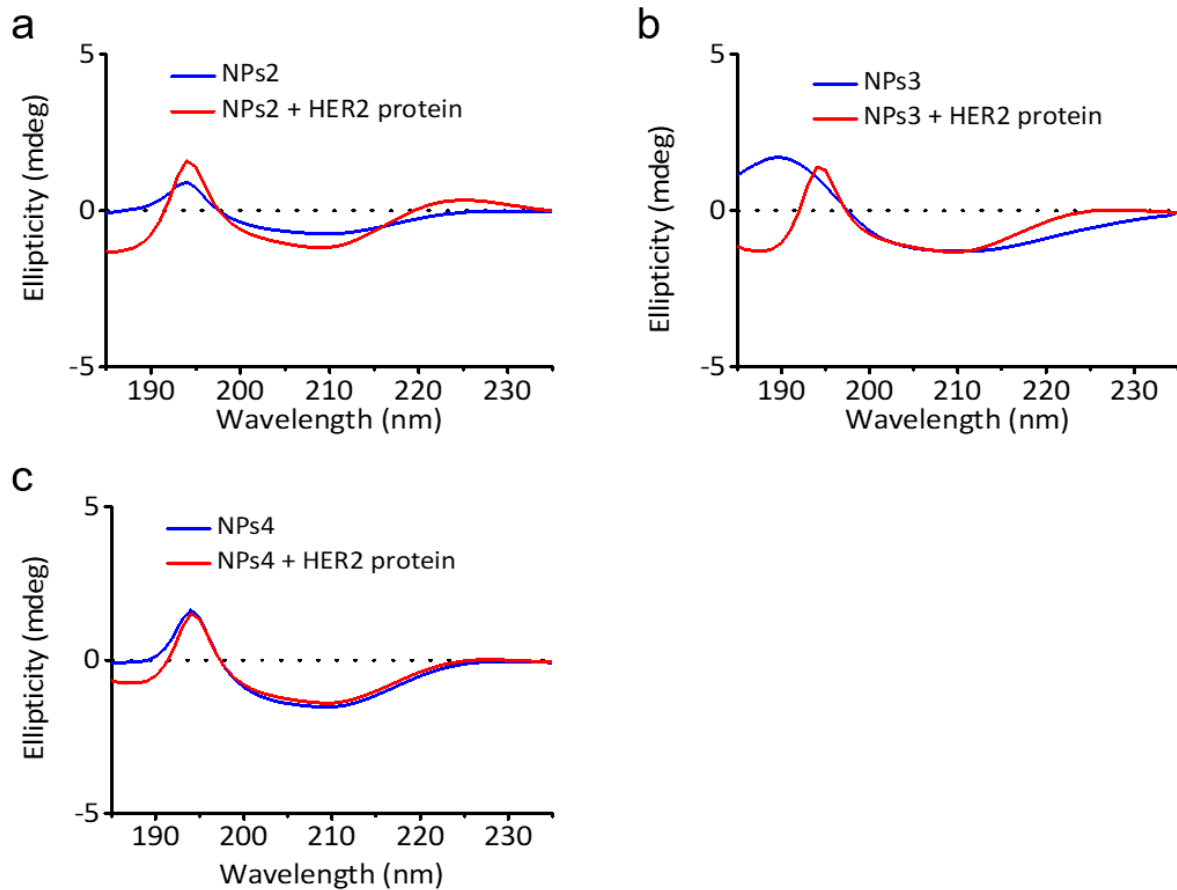
Supplementary Fig. 4. Effect of HER2 protein/peptide ligand ratio on fibrillar transformation. TEM images and particle size measurements of NPs1 were obtained after incubation with soluble HER2 protein for 24 h in PBS solution. NPs1 concentration was maintained constant at 20 μ M. The scale bar is 200 nm. The HER2 protein/peptide ligand ratio is labeled for each micrograph. Experiments were repeated three times.



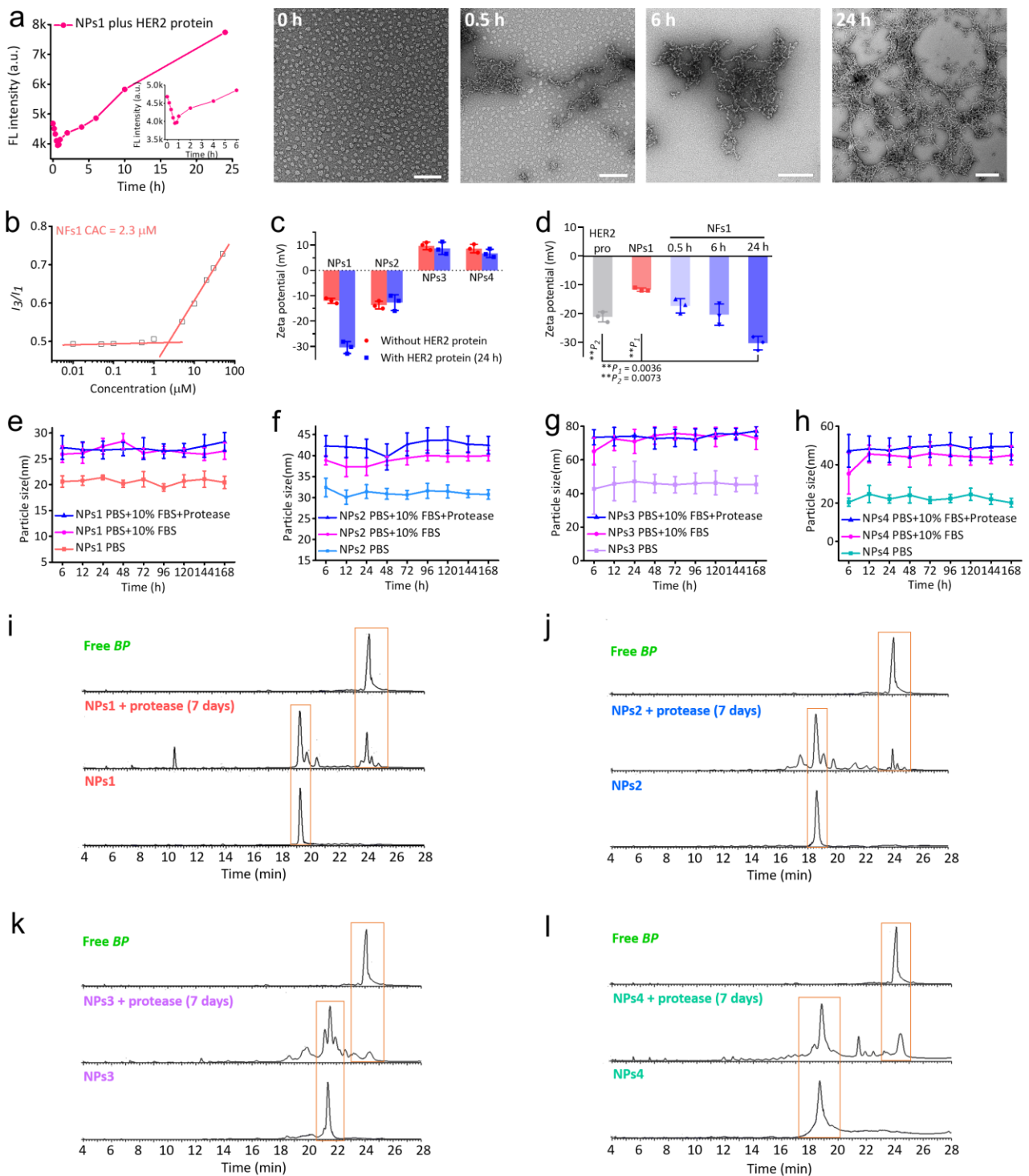
Supplementary Fig. 5. TEM images of freshly prepared NPs1 and NPs1 after 24 h in PBS solution. The concentration of NPs1 used in the experiment was 20 μM . The scale bar is 100 nm. Experiments were repeated three times.



Supplementary Fig. 6. TEM images and size distribution of initial NPs2-4 and NPs2-4 interaction with HER2 protein for 24 h. The concentration of NPs2-4 used in the experiment was 20 μM . The molar ratio of HER2 protein/peptide ligand was approximately 1:1000. The scale bar is 100 nm. Experiments were repeated three times.

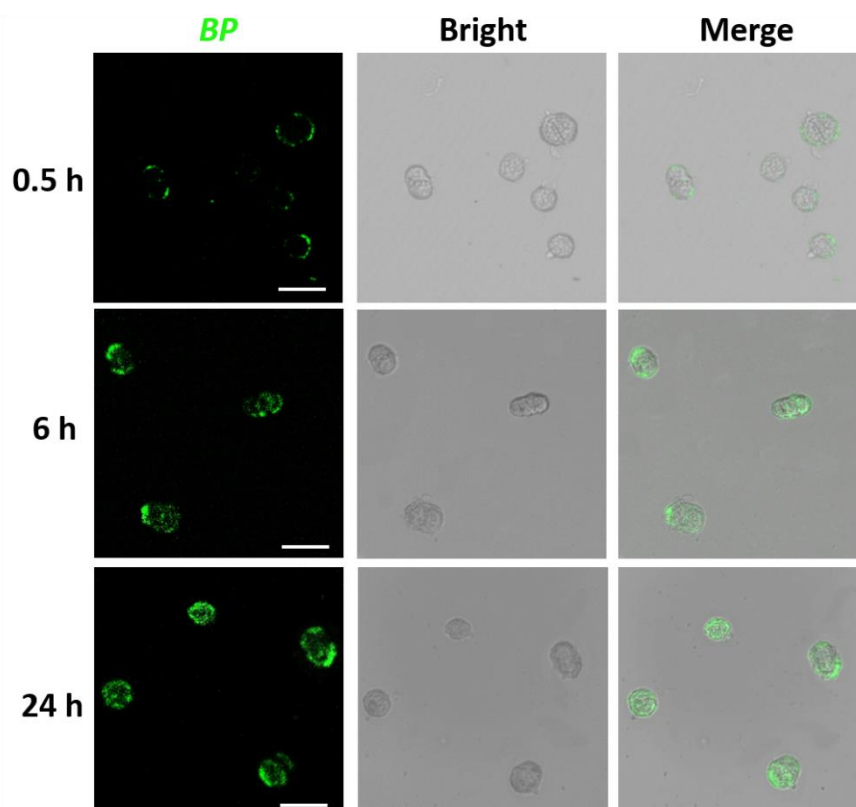


Supplementary Fig. 7. CD spectra of initial NPs2-4 and NPs2-4 interaction with HER2 protein for 24 h. Experiments were repeated three times.

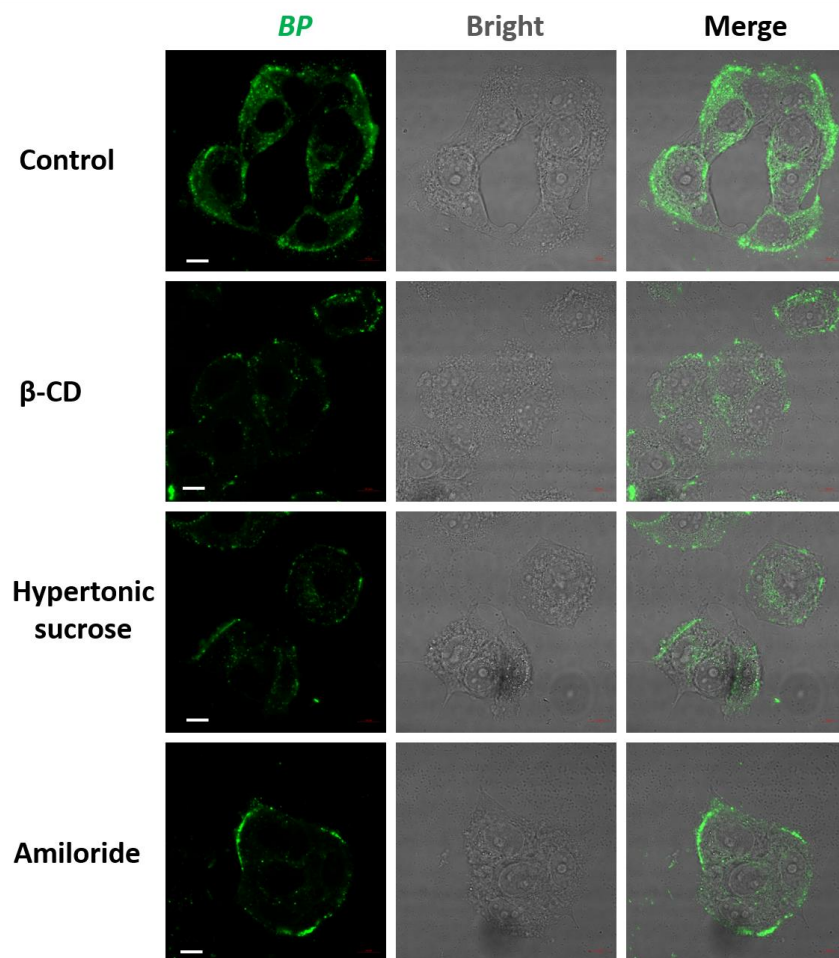


Supplementary Fig. 8. a, Fluorescence signal change and TEM images with the interaction of NPs1 and HER2 protein at the different time points. The molar ratio of HER2 protein/peptide ligand was approximately 1:1000. Experiments were repeated three times. The fluorescence intensity of BP in NPs1 dropped about 15.6% 40 min after addition of HER2, but turned around and increased as transformation to NFs1 progressed, and eventually reached about 65.2% increase by 24 h. One plausible explanation for this interesting observation is that the packing density of BP or TPM1 in the fibrillar networks (NFs1 at 24 h) was significantly higher than that in the initial spherical structure (NPs1). However, during the initial transformation process when the spherical NPs1 were exposed to HER2,

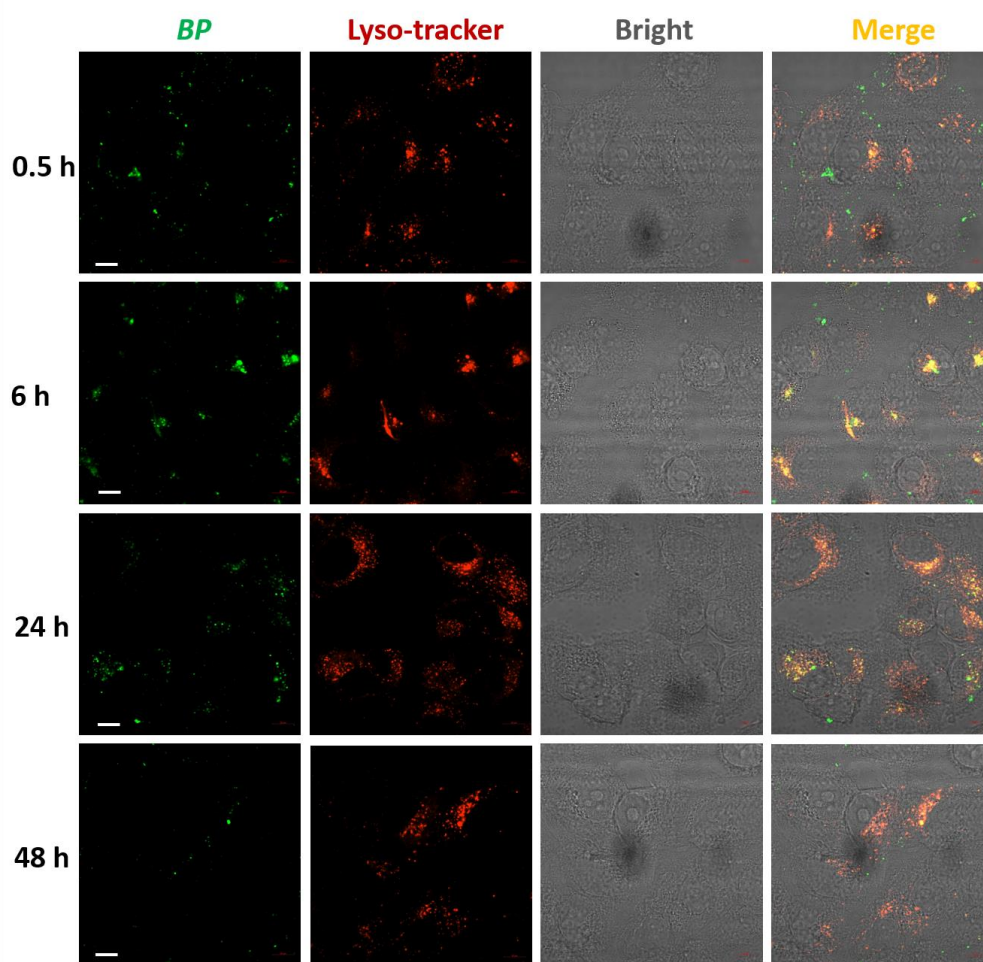
there was a transient relaxation in the packing density during the first 40 minutes prior to re-organization into the more densely packed nano-fibrillar network. The scale bar in **a** is 100 nm. **b**, The critical aggregation concentration of NFs1 was determined to be 2.3 μM . Experiments were repeated three times. **c**, zeta potential variation of NPs1-4 with or without HER2 protein after 24 h. Data are presented as the mean \pm s.d., $n = 3$ independent experiments. **d**, zeta potential variation of NPs1 as interaction with HER2 protein over time. The molar ratio of HER2 protein/peptide ligand was approximately 1:1000. Data are presented as the mean \pm s.d., $n = 3$ independent experiments. The statistical significance was calculated *via* one-way analysis of variance (ANOVA) with a Tukey post-hoc test. $**P < 0.01$. **e-h**, Nanoparticle stability of NPs1-4 in serum and protease (PBS solution of pH 7.4 with/without 10% FBS and protease) at 37 $^{\circ}\text{C}$ was measured by dynamic light scattering. Data are presented as the mean \pm s.d., $n = 3$ independent experiments. **i-l**, HPLC traces of NPs1-4 (300 μM) after 7 days incubation in protease solution (2 mg/mL) at 37 $^{\circ}\text{C}$ (pH = 7.4) and the control free bis-pyrene (*BP*) dye. Experiments were repeated independently for three times. Some transforming peptides did degrade but significant portion of the transforming peptides remained intact after 7 days at 37 $^{\circ}\text{C}$, indicating good serum stability and proteolytic stability.



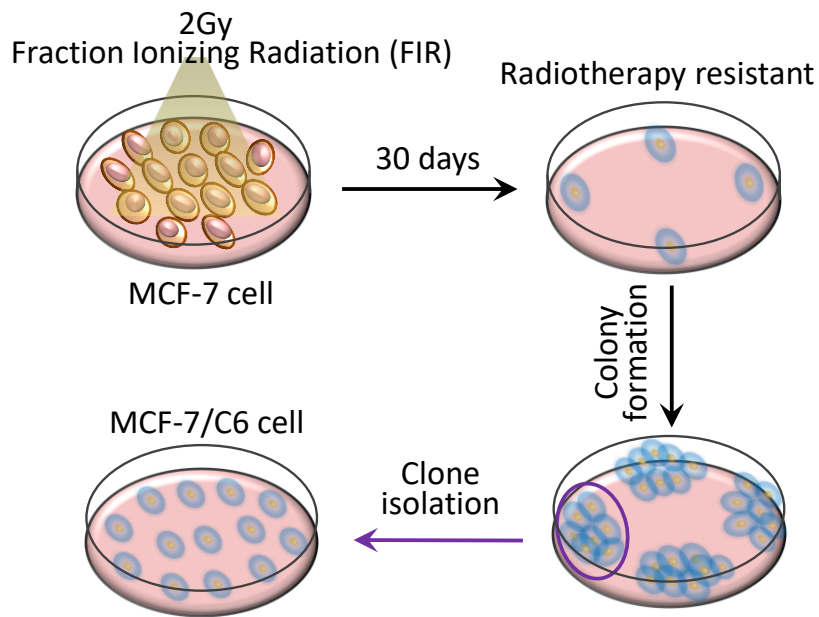
Supplementary Fig. 9. Cellular fluorescence distribution images of NPs1 incubation with low HER2 expression MCF-7 cells over time (0.5, 6, 24h). The concentration of NPs1 used was 50 μM ; scale bar is 50 μm . Experiments were repeated three times.



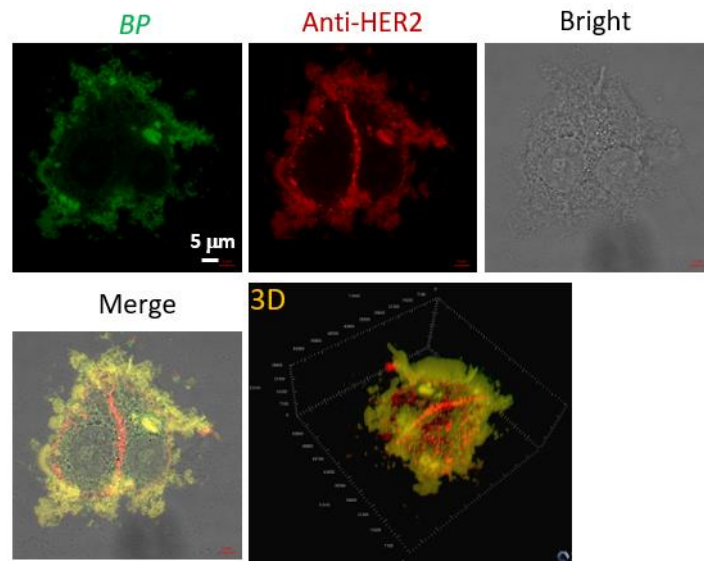
Supplementary Fig. 10. Cell uptake pathway detection. CLSM images of MCF-7 cells incubated with NPs1 (50 μ M) in the presence of various endocytosis inhibitors, such as amiloride (2 mM), β -CD (5 mM), and hypertonic sucrose (450 mM), respectively. The scale bar is 10 μ m. Experiments were repeated three times.



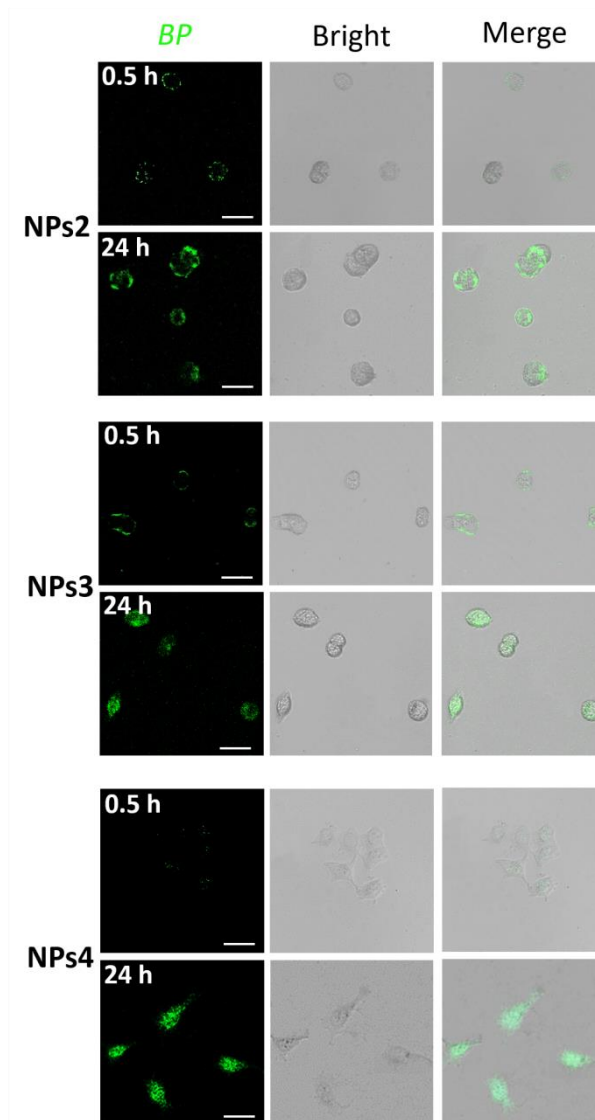
Supplementary Fig. 11. Cellular fluorescence distribution and fluorescence conversion process images of NPs1 incubation with low HER2 expression MCF-7 cells over time (0.5, 6, 24 and 48 h). Experiments were repeated three times. The concentration of NPs1 was 20 μM . Co-localization of BP green signal and Lyso-tracker red signal was observed at 6 h, but the green signals continued to decrease over the next two days. The result is consistent with the notion that NPs1 taken up by cell *via* endocytosis was dissociated and eventually degraded at the lysosomes without significant toxicity to cells at 48 h. The scale bar is 10 μm .



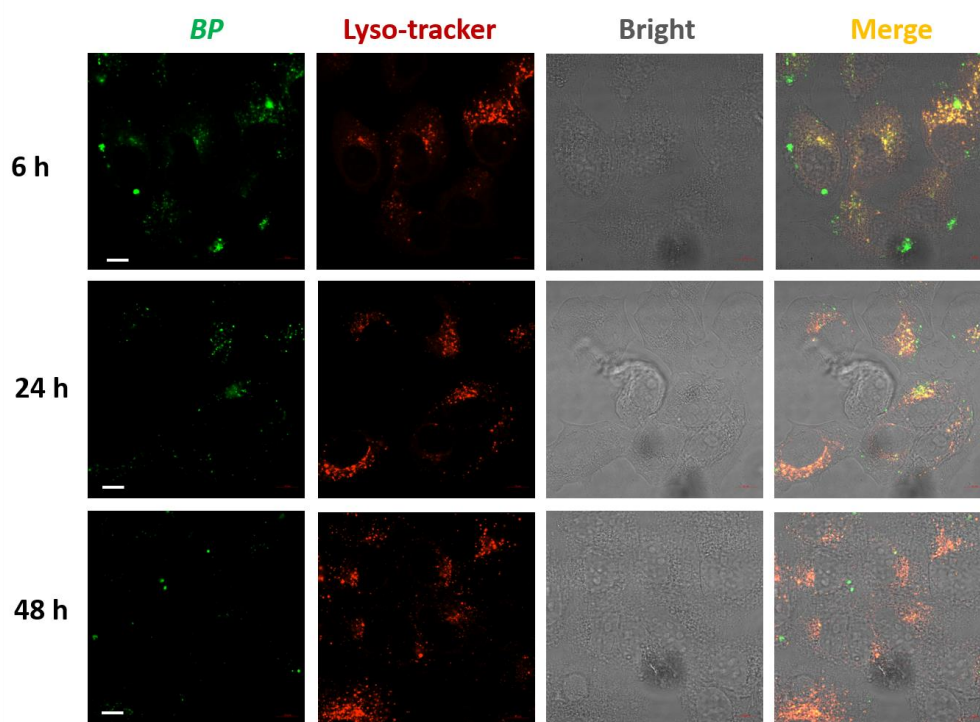
Supplementary Fig. 12. Schematic illustration of the inducing process of MCF-7/C6 cells *via* fraction ionizing radiation (FIR) from MCF-7 cells.



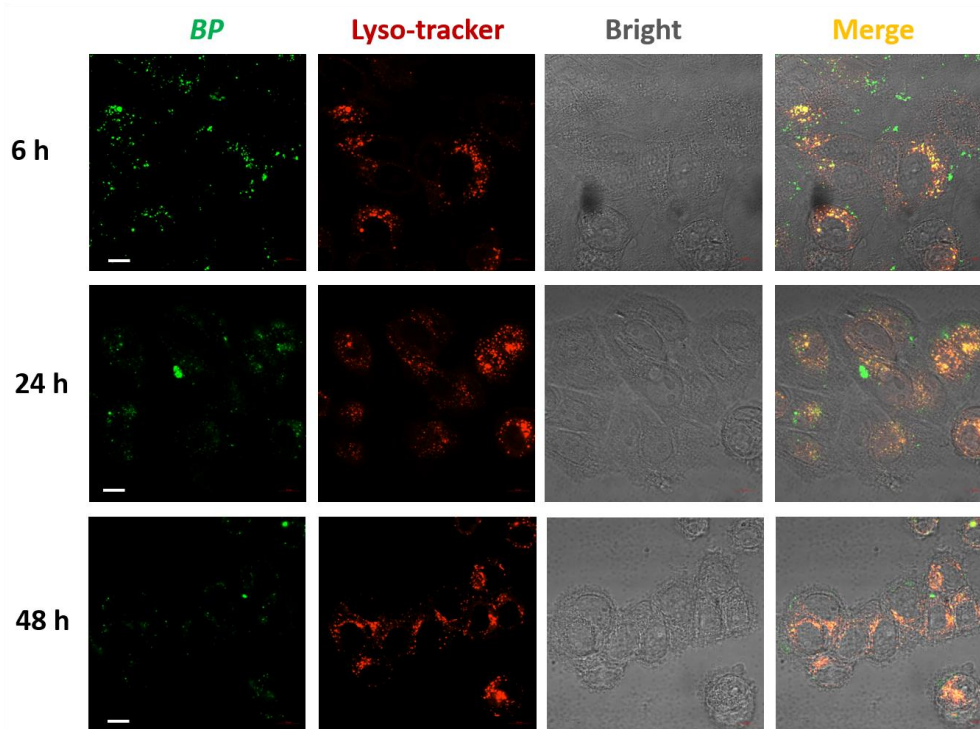
Supplementary Fig. 13. 2D and 3D images of fluorescence binding distribution for NPs1 and anti-HER2 antibody (29D8 rabbit Ab and HER2 peptide of NPs1 recognize different epitopes of HER2 receptor) on the cell membrane of MCF-7/C6 cells for 6 h. Anti-HER2 antibody was used to label HER2 receptors on the cell membrane. Experiments were repeated three times. The concentration of NPs1 used was 50 μM.



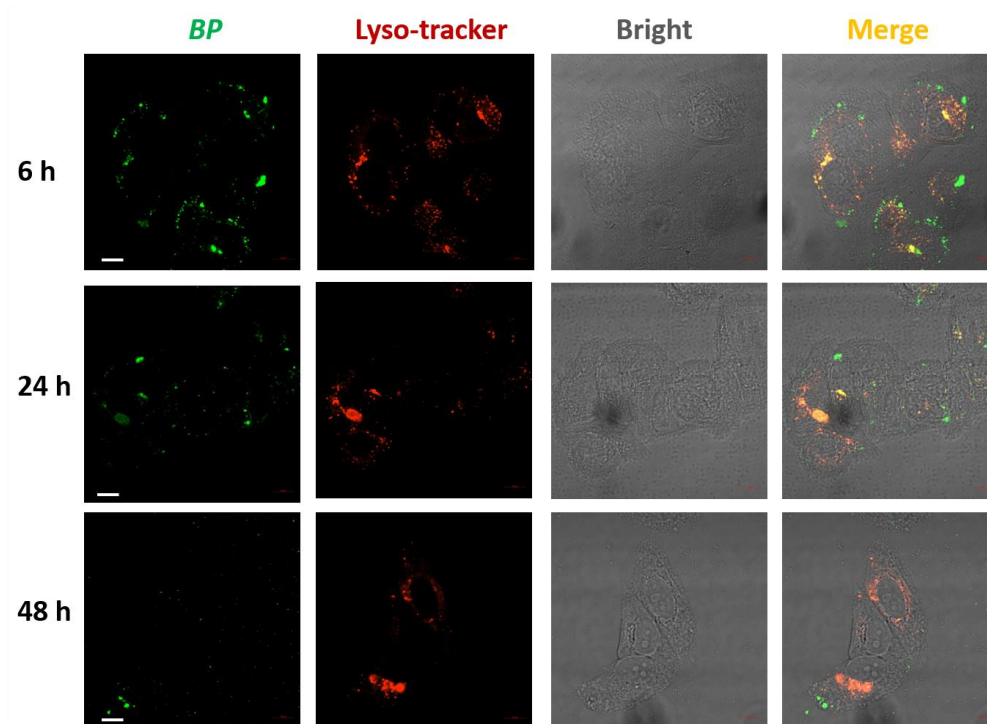
Supplementary Fig. 14. Cellular fluorescence distribution images of NPs2-4 interaction with MCF-7/C6 cells at two different time points (0.5 and 24 h). Experiments were repeated three times. The concentration of NPs2-4 used was 50 μ M. Scale bar is 50 μ m.



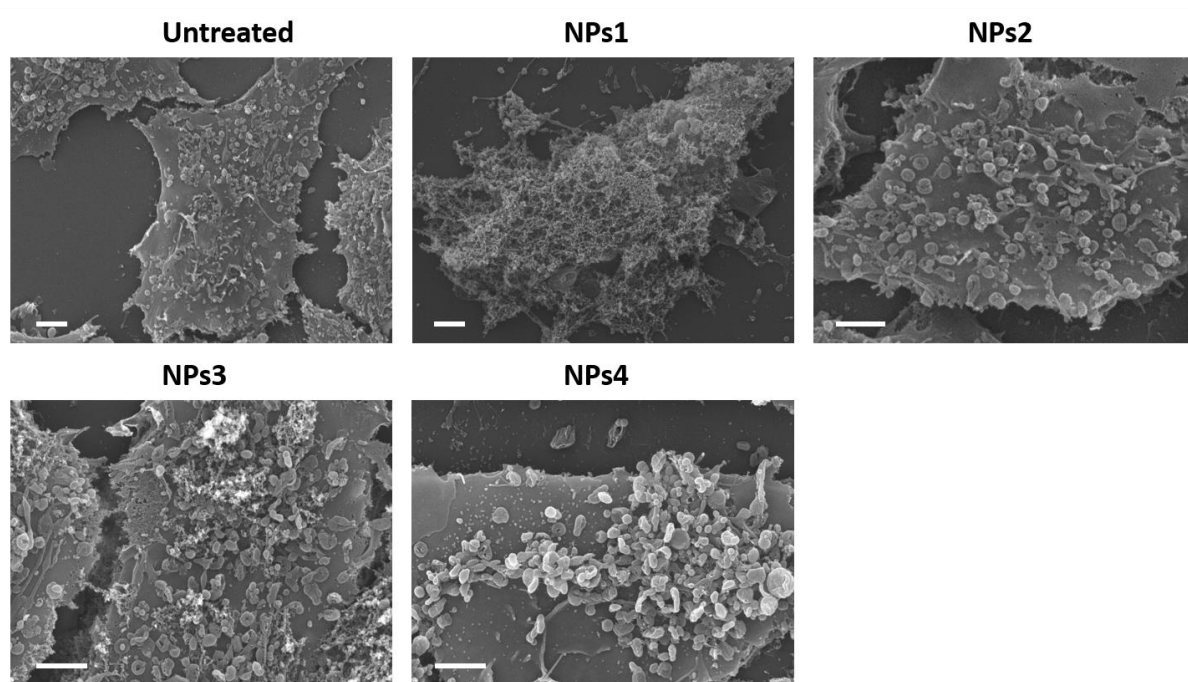
Supplementary Fig. 15. Cellular fluorescence distribution and fluorescence conversion process images of NPs2 incubation with MCF-7/C6 cells over time (6, 24 and 48 h). Experiments were repeated three times. The concentration of NPs2 used was 20 μ M. Based on the fluorescence conversion process, most of the internalized NPs2 were degraded by the lysosomes, without significant toxicity to cells at 48 h. The scale bar is 10 μ m.



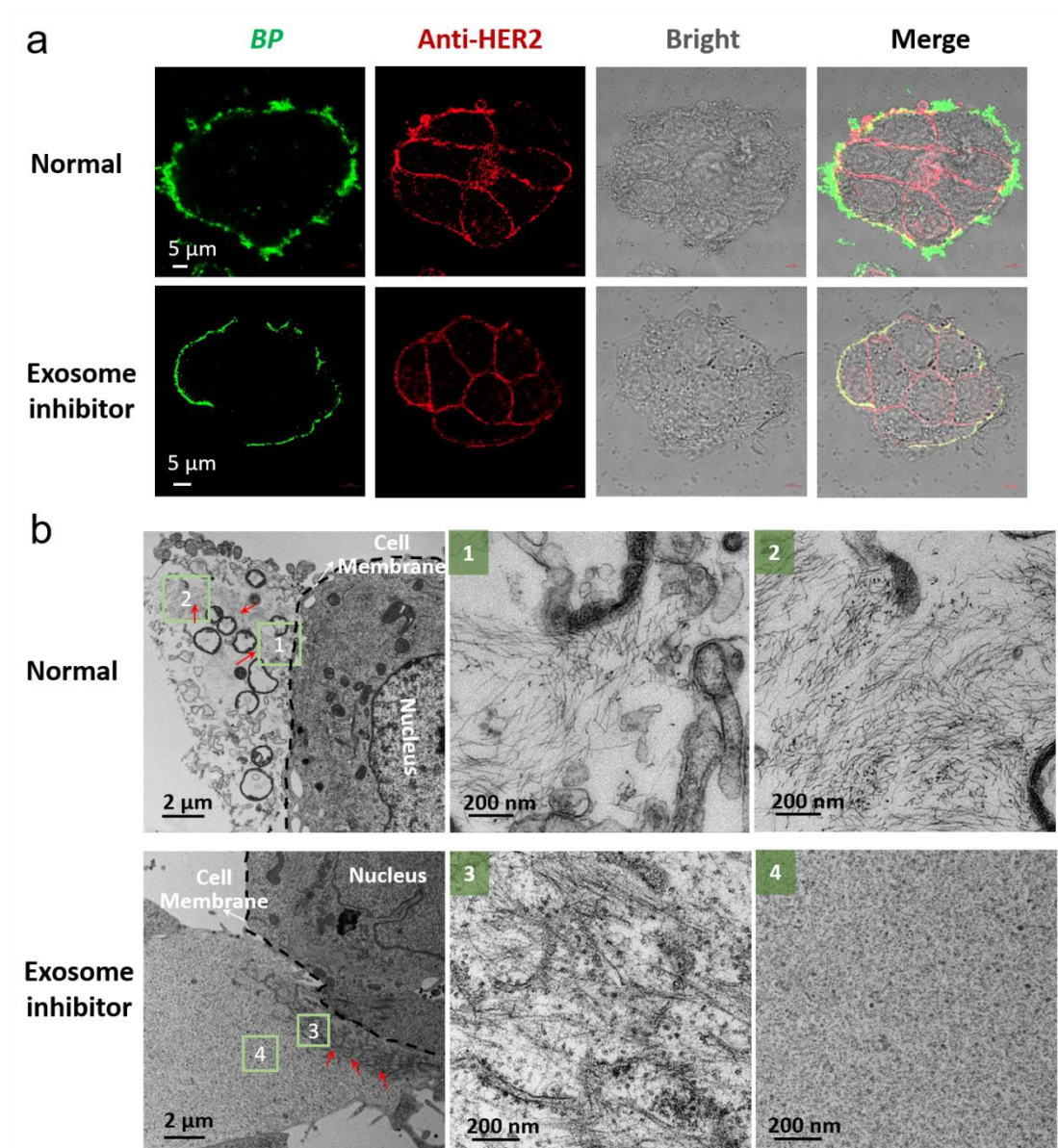
Supplementary Fig. 16. Cellular fluorescence distribution and fluorescence conversion process images of NPs3 incubation with MCF-7/C6 cells over time (6, 24 and 48 h). Experiments were repeated three times. The concentration of NPs3 used was 20 μ M. Based on the fluorescence conversion process, most of the internalized NPs3 were degraded by the lysosomes without significant toxicity to cells at 48 h. The scale bar is 10 μ m.



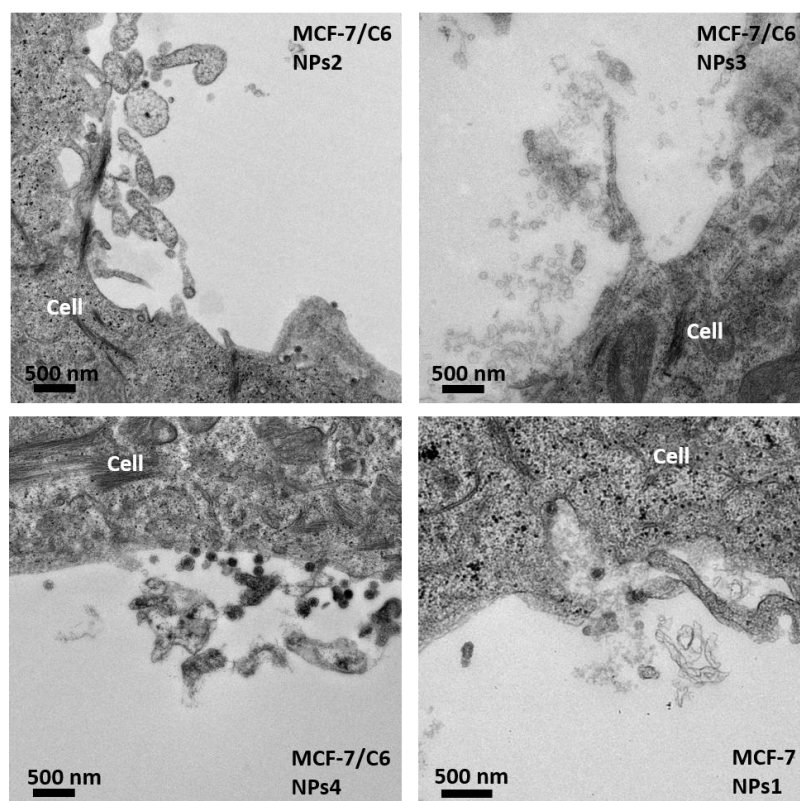
Supplementary Fig. 17. Cellular fluorescence distribution and fluorescence conversion process images of NPs4 incubation with MCF-7/C6 cells over time (6, 24 and 48 h). Experiments were repeated three times. The concentration of NPs4 used was 20 μ M. Based on the fluorescence conversion process, most of the internalized NPs4 were degraded in lysosome without significant toxicity to cells at 48 h. The scale bar is 10 μ m.



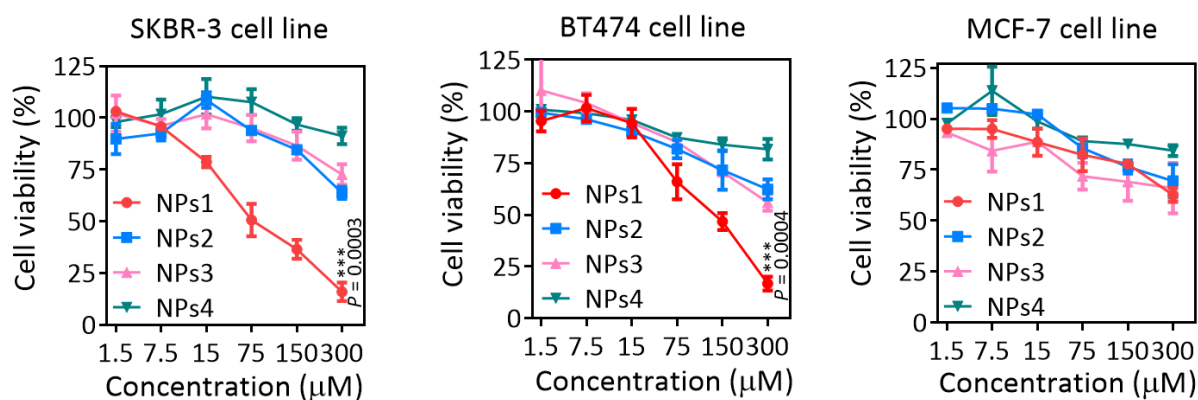
Supplementary Fig. 18. SEM images of untreated MCF-7/C6 cells and cells treated with NPs1-4 for 24 h. The concentration of NPs1-4 used was 50 μM . Experiments were repeated three times. The scale bar is 3 μm .



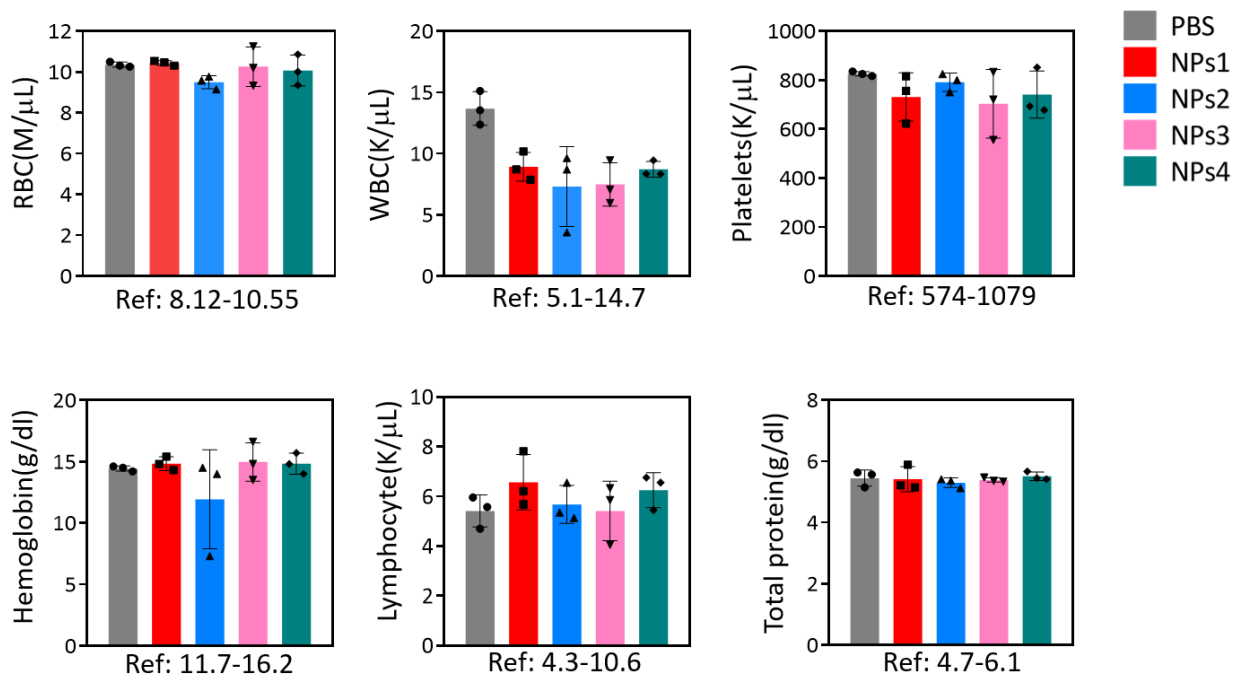
Supplementary Fig. 19. a, Fluorescent images of the nanofibrillar network formation on the cell surface of MCF-7/C6 cell cluster after incubation with NPs1 for 24 h, in the presence or absence of exosome inhibitor (GW4869, 2 μ M) for one hour prior to addition of NPs1. HER2 antibody (29D8 rabbit Ab) was used to label HER2 receptors on the cell membrane. A much thinner green fluorescence signal layer was observed in the presence of exosome inhibitor. Experiments were repeated three times. **b**, TEM images of MCF-7/C6 cells treated by NPs1 with or without exosome inhibitor for 24 h. The red arrows show fibrillar network. Experiments were repeated three times. The concentration of NPs1 used was 50 μ M. Luxuriant fibrillar networks in normal group was detected in both regions adjacent to and further away from the cell membrane (region 1 and 2). Fibrillar structures were found in abundance only in close proximity to the cell membrane (region 3), but not in region 4 in the group with exosome inhibitor.



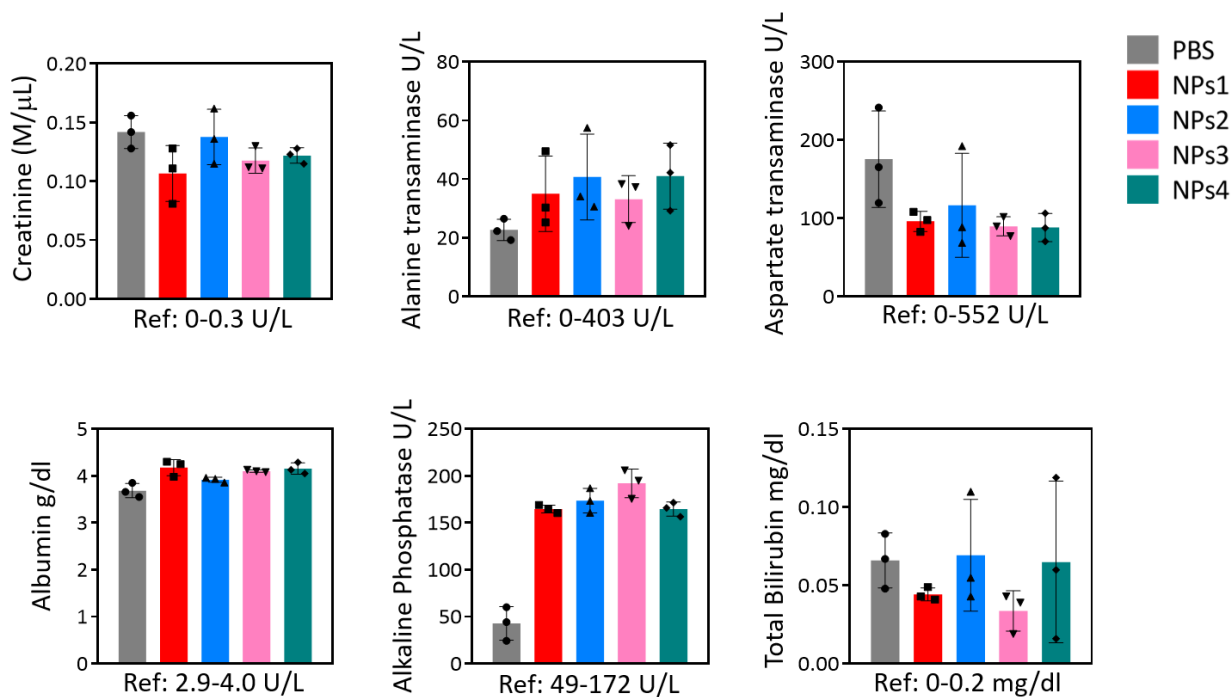
Supplementary Fig. 20. TEM images of MCF-7/C6 cells treated with NPs2-4 and MCF-7 cells treated with NPs1 for 24 h. The concentration of NPs1-4 used was 50 μM . Experiments were repeated three times.



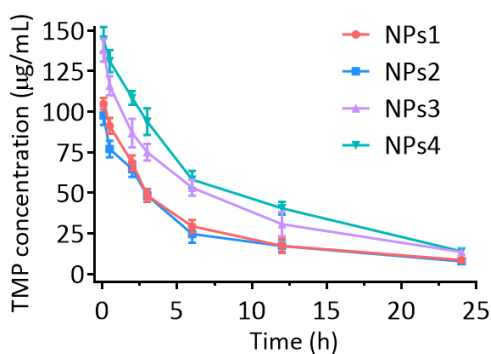
Supplementary Fig. 21. The viability of SKBR-3, BT474 and MCF-7 cells incubated with NPs1-4 at different concentrations for 48 h. Data are presented as the mean \pm s.d., $n=3$ independent experiments. The statistical significance was calculated *via* one-way ANOVA with a Tukey post-hoc test. *** $P < 0.001$.



Supplementary Fig. 22. Blood test parameters in terms of red blood cells (RBC), white blood cells (WBC), platelets, hemoglobin, lymphocyte and total protein of healthy Balb/c mice, after 8 q.o.d. intravenous injections of NPs1-4 (8 mg/kg per injection). Data are presented as the mean \pm s.d., $n = 3$ independent experiments.

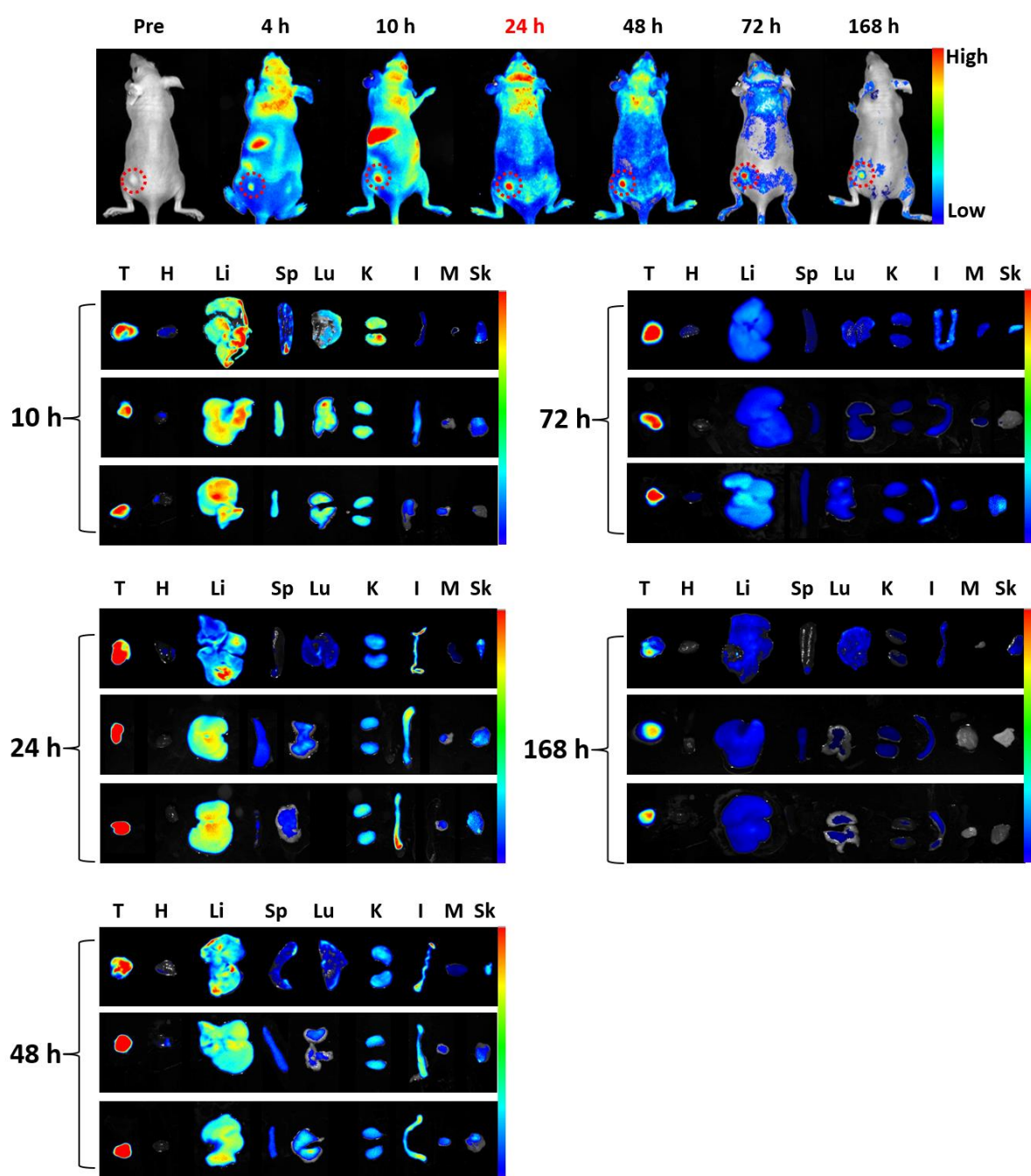


Supplementary Fig. 23. Blood test parameters in terms of liver function creatinine, alanine transaminase, aspartate transaminase, albumin, alkaline phosphatase, total bilirubin of healthy Balb/c mice after 8 q.o.d. intravenous injection of NPs1-4 (8 mg/kg per injection). Data are presented as the mean \pm s.d., $n = 3$ independent experiments.

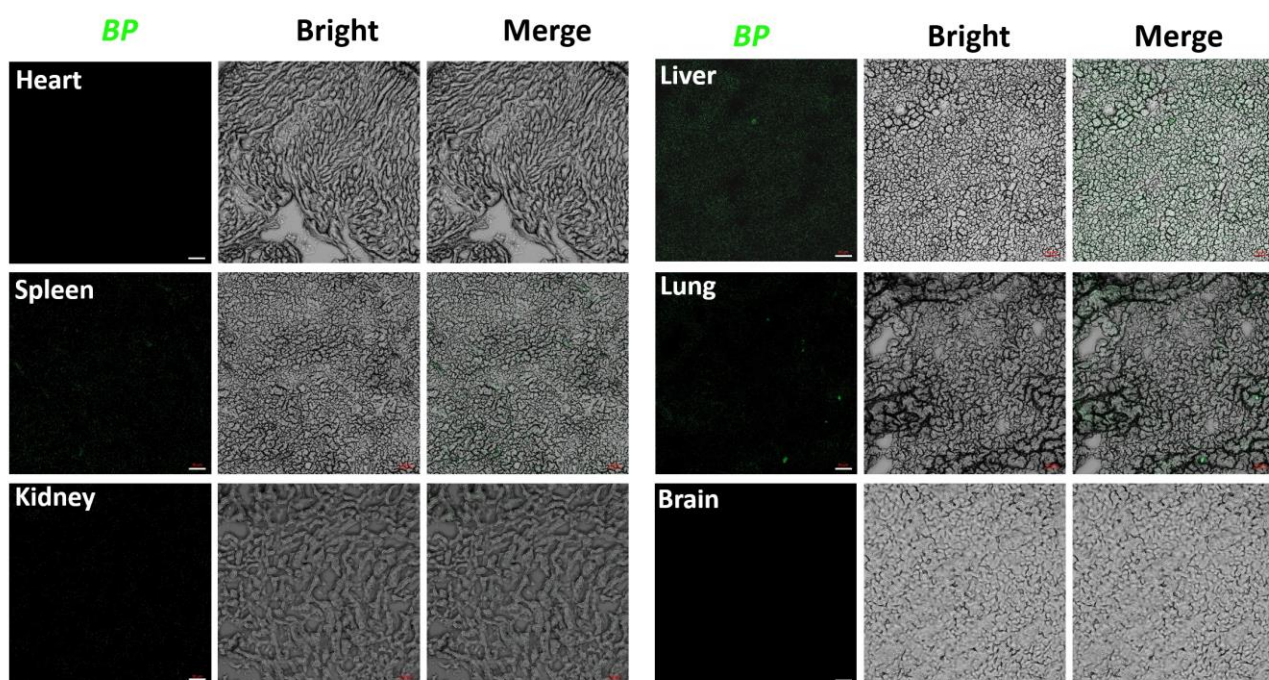


Group	C-max (μ g/mL)	AUC	T-half (α)	T-half (β)
NPs1	104.827	800.273	1.9491	16.9976
NPs2	96.484	726.787	1.9288	14.7398
NPs3	129.528	1198.621	2.1894	20.1684
NPs4	148.138	1320.137	2.2522	22.2719

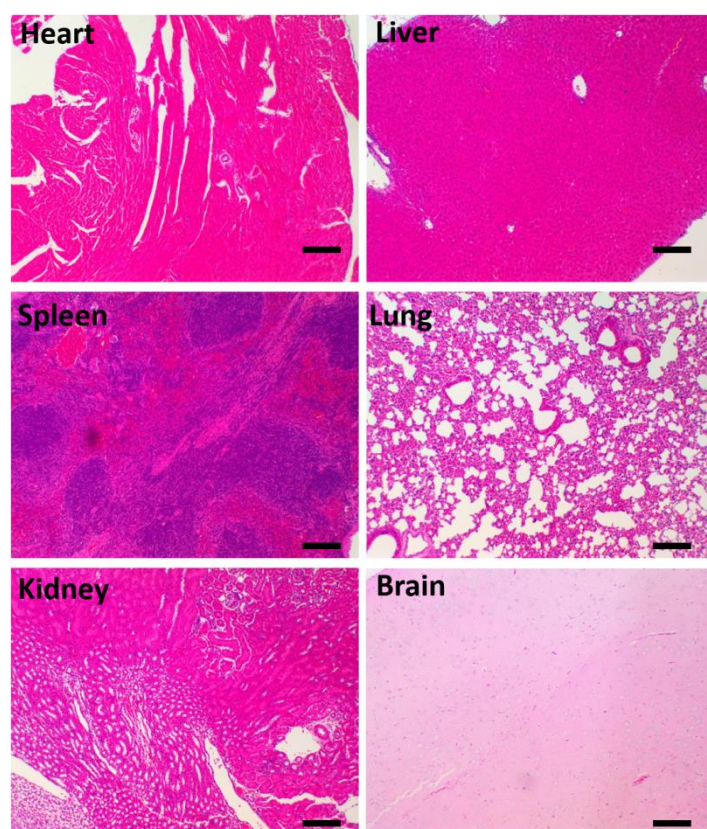
Supplementary Fig. 24. *In vivo* blood pharmacokinetics and parameter of NPs1-4 (Data are presented as the mean \pm s.d., $n = 3$ independent experiments). The C-max, AUC and $T_{1/2}$ (hours) were calculated by Kinetica 5.0.



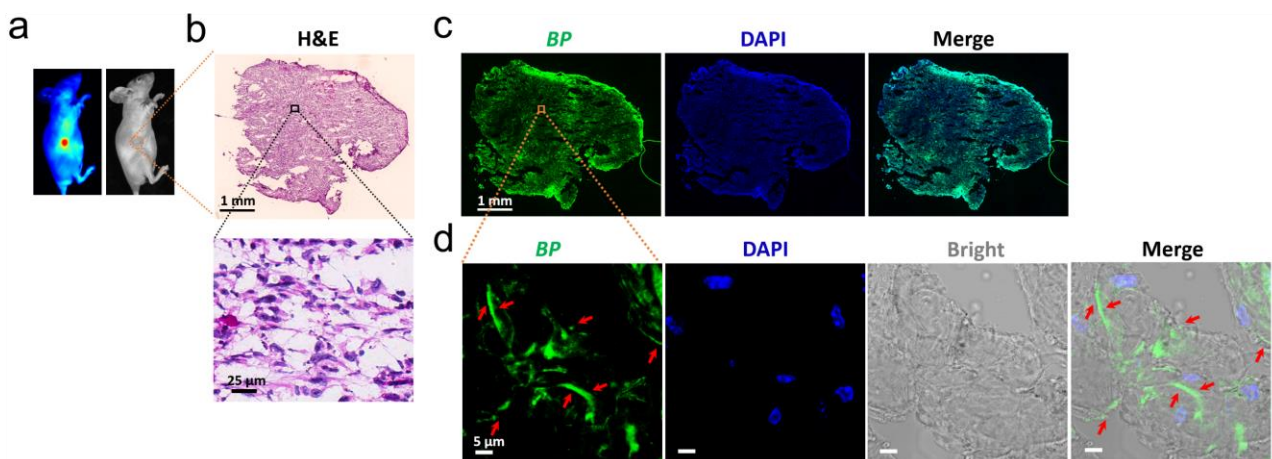
Supplementary Fig. 25. Time-dependent *in vivo* and *ex vivo* fluorescence images of tumour tissue and major organs at different time point after i.v. injection of NPs1, in MCF-7/C6 tumour model ($n = 3$). The concentration of NPs1 used was 8 mg/kg.



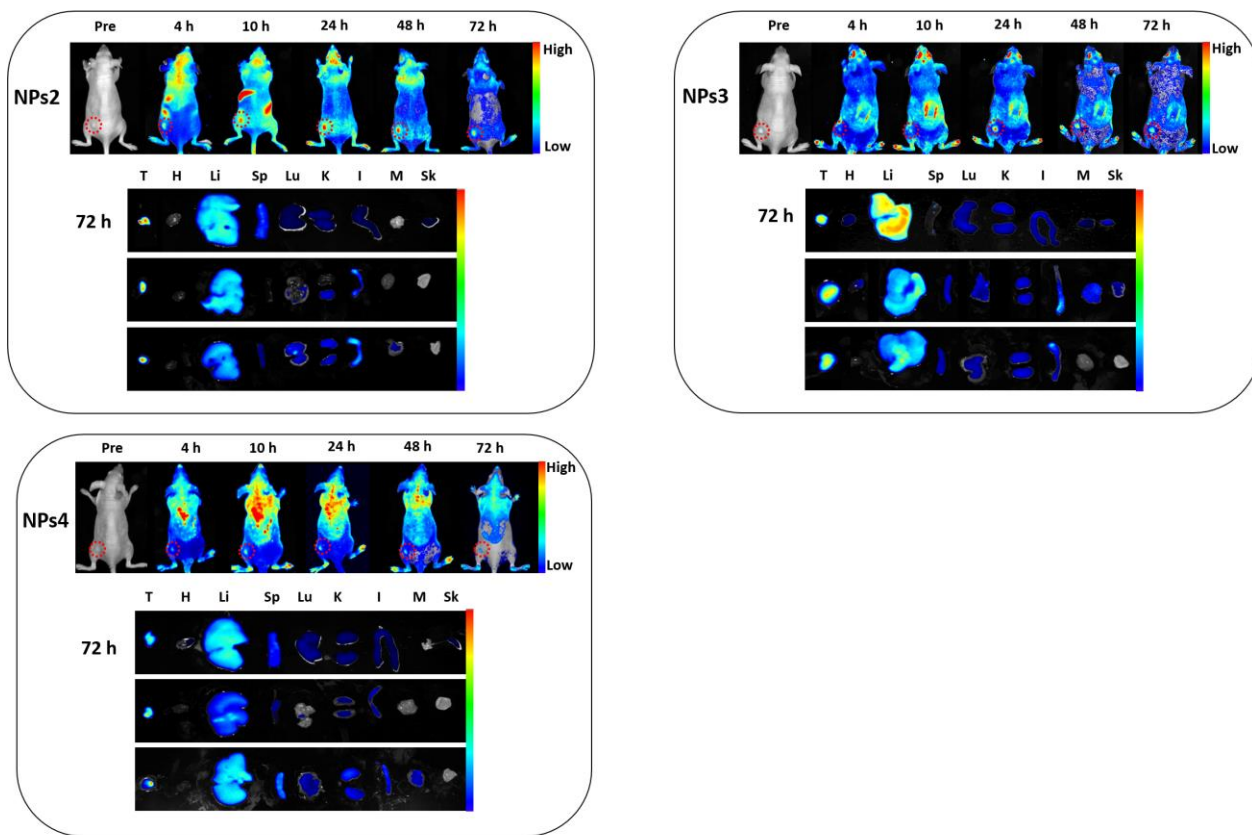
Supplementary Fig. 26. The fluorescent images of NPs1 in tissue sections of main organs at 72 h post-injection (The concentration of NPs1 used was 8 mg/kg; green color: *BP* of NPs1; scale bar is 50 μ m). Experiments were repeated three times.



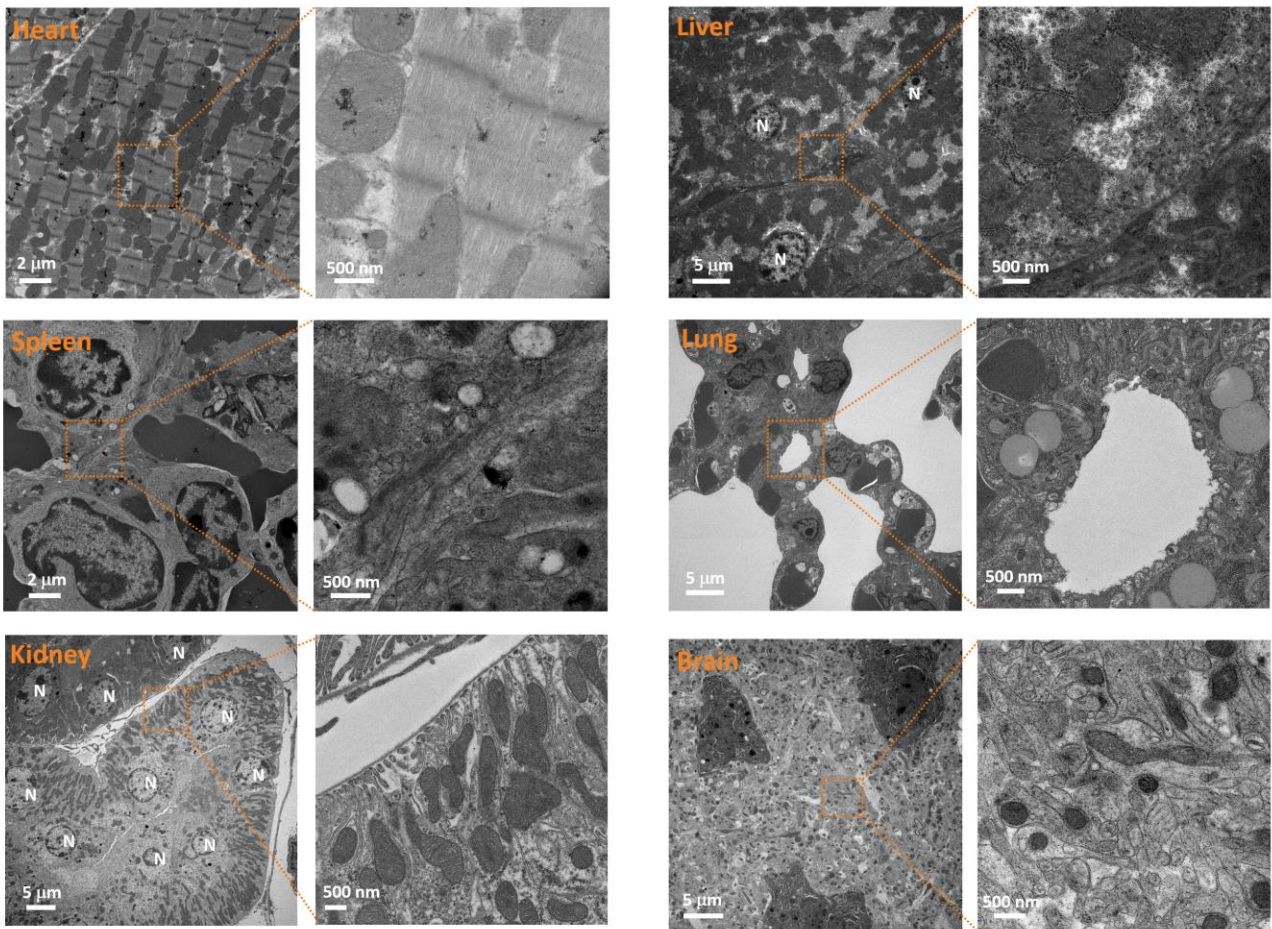
Supplementary Fig. 27. H&E stain of main organs did not show any systemic toxicity caused by NPs1 72 h after i.v. injection (The concentration of NPs1 used was 8 mg/kg). Experiments were repeated three times. The scale bar is 200 μm .



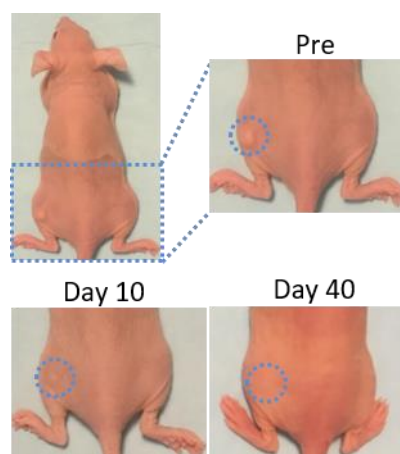
Supplementary Fig. 28. **a**, *In vivo* fluorescence images of tumour tissue at 72 h after i.v. injection of NPs1 in MCF-7/C6 tumour model. The concentration of NPs1 used was 8 mg/kg. Experiments were repeated three times. **b,c**, **(b)** The H&E stain images and **(c)** fluorescence distribution images of NPs1 in whole excised tumour tissue at 72 h post-injection (In **b**, green color: *BP* of NPs1; blue color: DAPI). **d**, An enlarged detailed outline of the *BP* fluorescence distribution of **c**. In **d**, most of the green fluorescence were observed in the cytoskeleton or the edge of the cell membrane, as indicated by the red arrow, indicating that NPs1 could transform into fibrillar-structures on the cell membrane *in vivo*, which was consistent with TEM data on tumour tissue treated by NPs1.



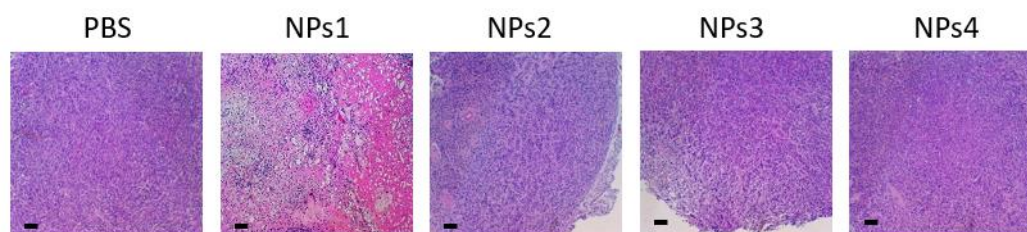
Supplementary Fig. 29. Time-dependent *in vivo* fluorescence images at different time point after i.v. injection of NPs2-4 and *ex vivo* images of tumour tissue and major organs at 72 h ($n = 3$). The concentration of NPs2-4 used were 8 mg/kg.



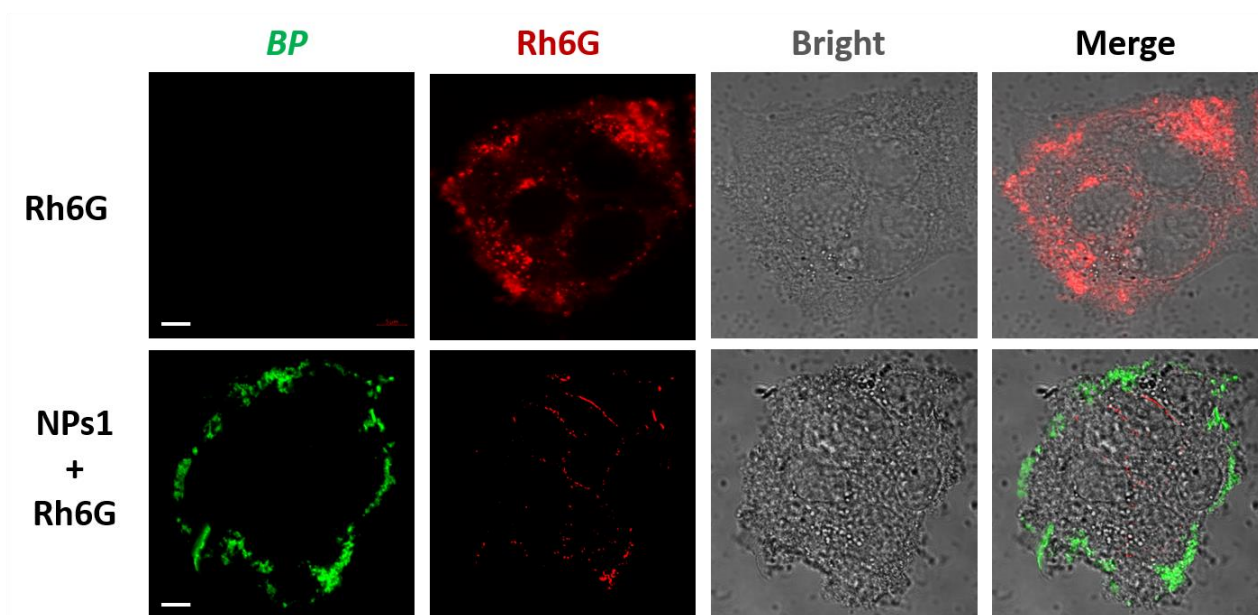
Supplementary Fig. 30. TEM images of distribution in main organs of NP1 at 72 h after i.v. injection. The concentration of NP1 used was 8 mg/kg. Experiments were repeated three times. The cell nuclei were labeled by the letter “N” in some of the micrographs.



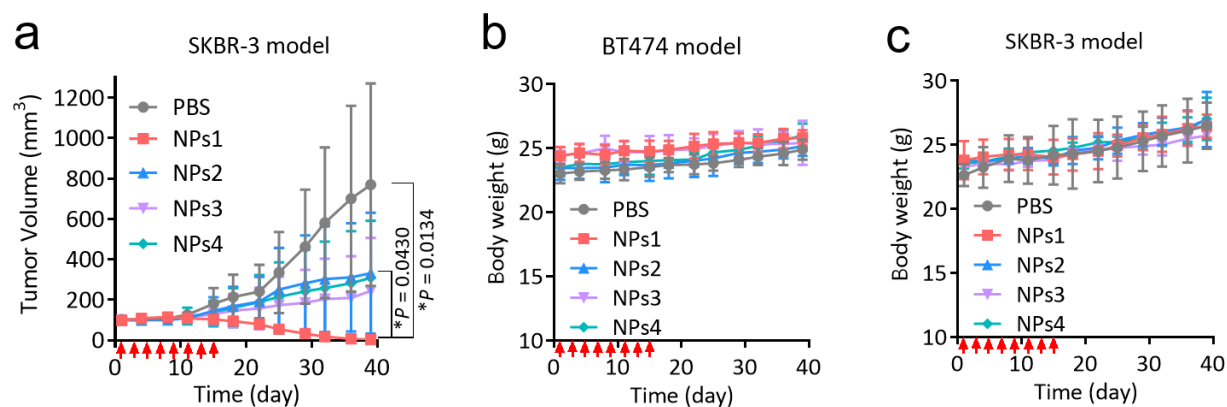
Supplementary Fig. 31. Representative photographs of MCF-7/C6 tumour volume variation in the group of mice treated with NPs1 for 40 days ($n = 8$). The concentration of NPs1 was 8 mg/kg per injection.



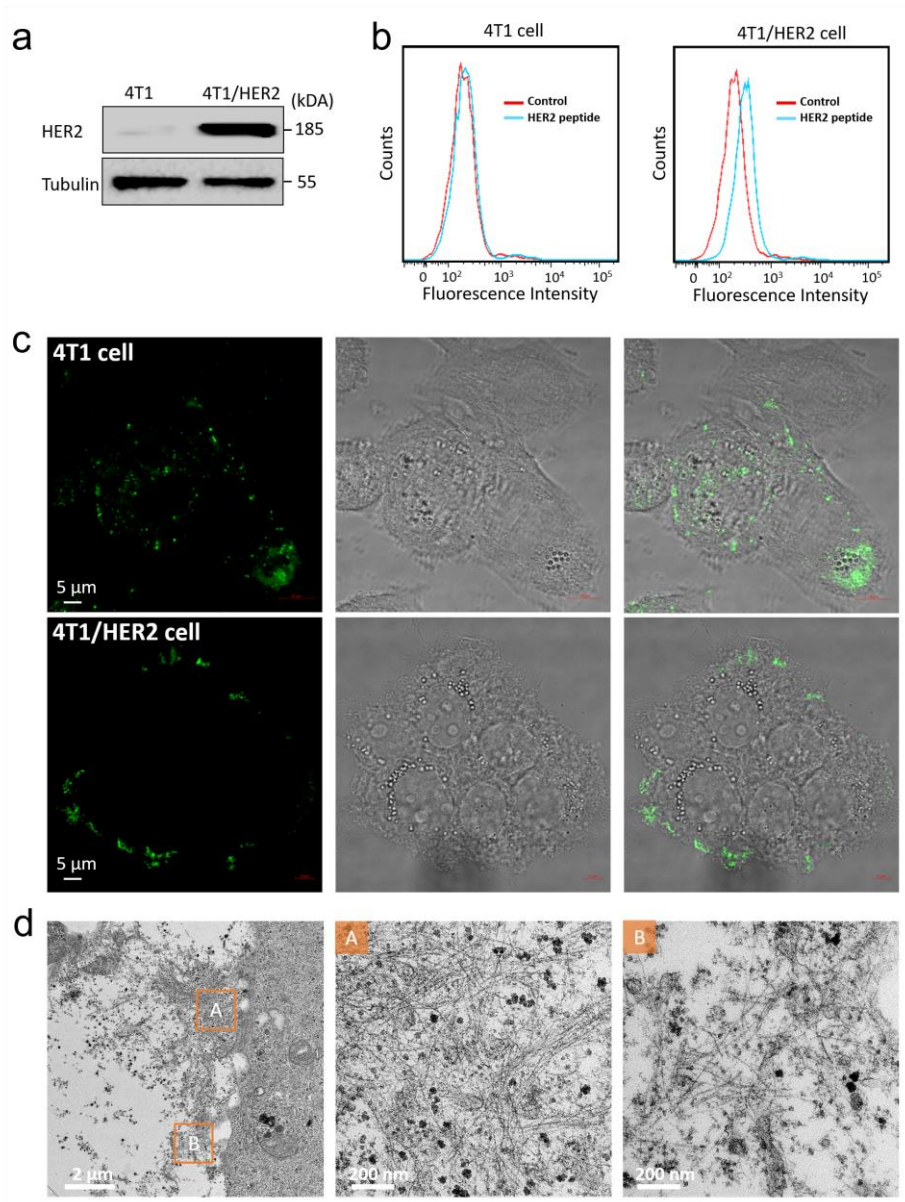
Supplementary Fig. 32. H&E images of MCF-7/C6 tumour tissues treated by different groups after injection three times ($n = 6$). Scale bar is 25 μm . The concentration of NPs1-4 were 8 mg/kg per injection.



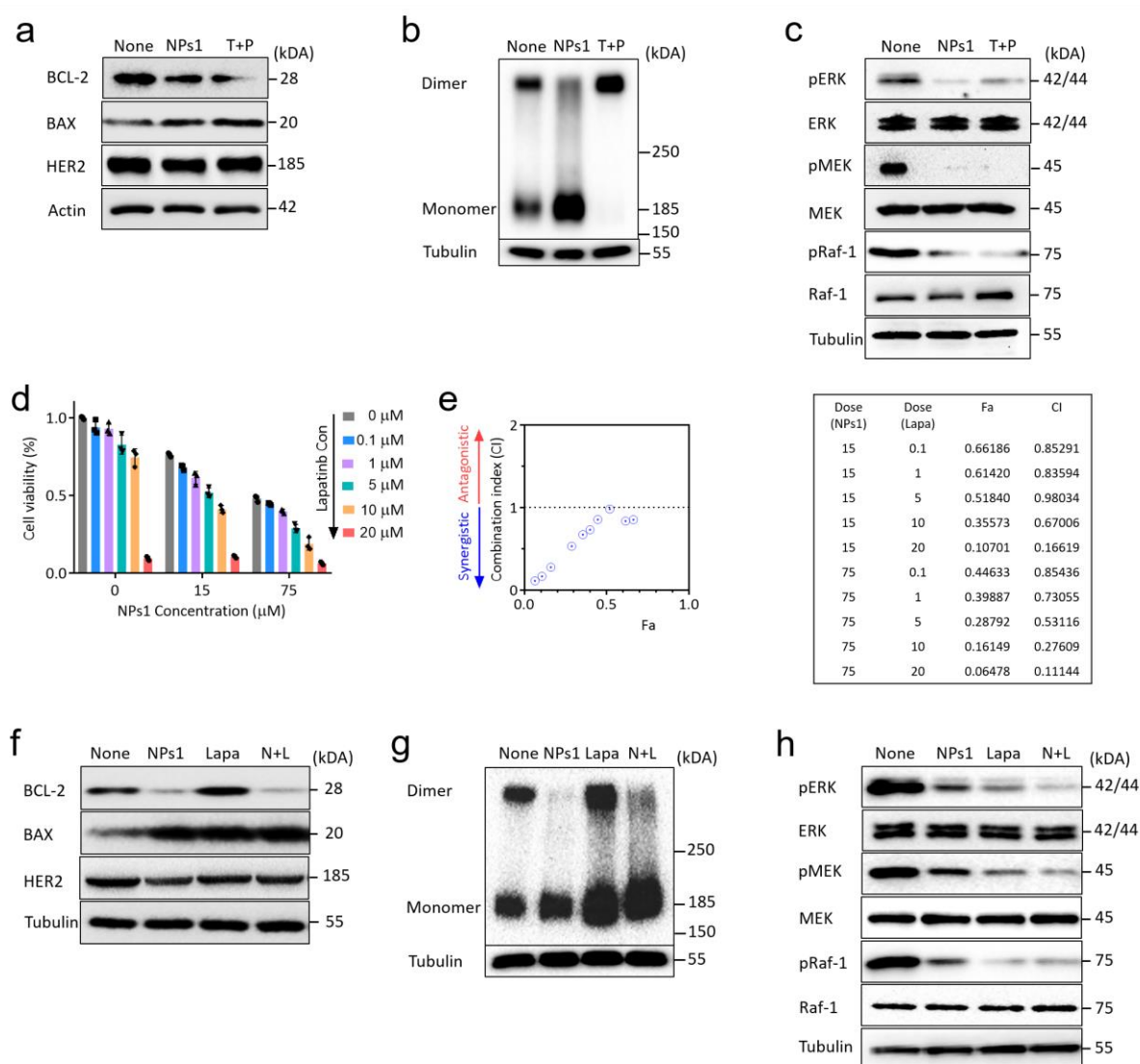
Supplementary Fig. 33. Fibrillar-networks on the cell surface was found to impair uptake of rhodamine 6G (Rh6G), a water-soluble dye. MCF-7/C6 cells were first incubated with NPs1 for 6 h, at which time fibrillar-structure would form on the cell surface. Rh6G was then added and the cells were washed after 30 minutes and prepared for CLSM. The concentration for NPs1 and Rh6G were 50 μ M and 2 μ M, respectively. Experiments were repeated three times. Scale bar is 5 μ m.



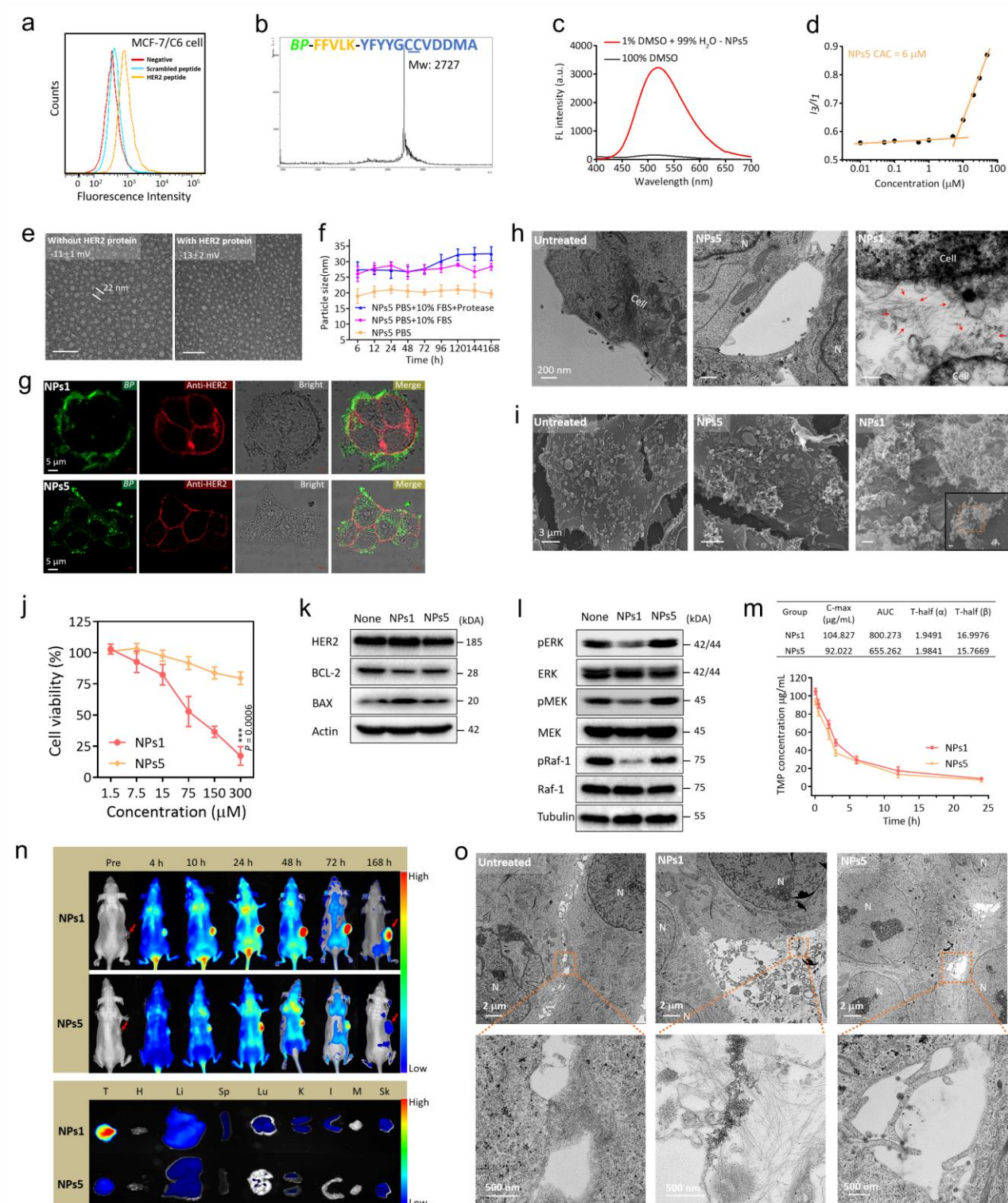
Supplementary Fig. 34. a, Observation on the anti-tumour effect in subcutaneous SKBR-3 tumour during the 40 days of treatment ($n = 6$ per group; the dose of NPs1-4 were 8 mg/kg per injection, q.o.d.; data are presented as the mean \pm s.d.). The statistical significance was calculated *via* one-way ANOVA with a Tukey post-hoc test. $*P < 0.05$. **b,c,** Body weight of mice bearing subcutaneous **(b)** BT474 tumour and **(c)** SKBR-3 tumour during the 40 days of treatment ($n = 6$ per group; data are presented as the mean \pm s.d.). Red arrows depict each single i.v. injection.



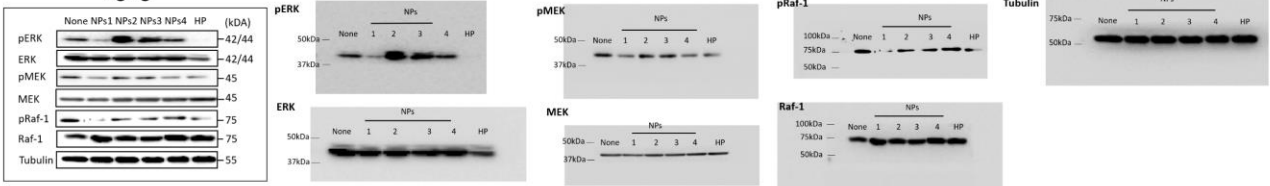
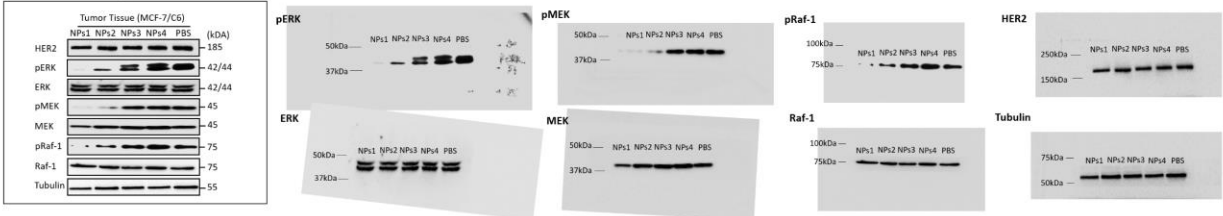
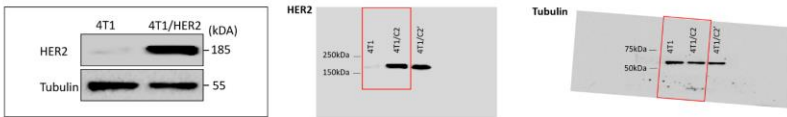
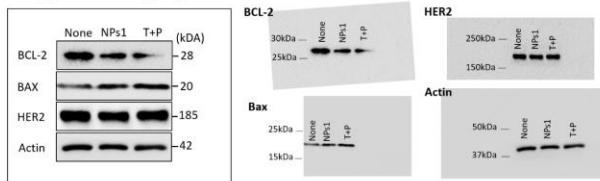
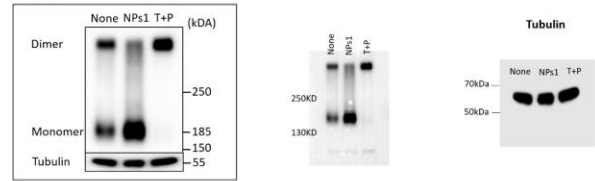
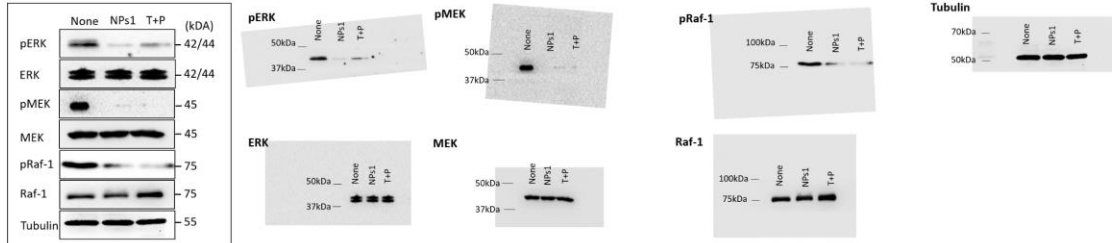
Supplementary Fig. 35. NP1 was able to undergo fibrillary transformation after co-culture with murine HER2 positive cancer cell line (4T1/HER2), which was derived and cloned from 4T1 murine breast cancer line that had undergone 30 days of FIR induction **a**, Western blot analysis of relative HER2 protein expression in 4T1 and 4T1/HER2 cells. Experiments were repeated three times. **b**, Biotinylated HER2 peptide (YCDGFYACYMDV, blue curve) and negative control (red curve) incubation with 4T1 and 4T1/HER2 cells were analyzed with flow cytometry. Experiments were repeated three times. **c**, Fluorescence binding distribution images of 4T1 and 4T1/HER2 cells after incubation with NP1 for 6 h, respectively. Experiments were repeated three times. **d**, TEM images of 4T1/HER2 cells after incubation with NP1 for 24 h. Experiments were repeated three times. The concentration of NP1 used was 50 μ M.



Supplementary Fig. 36. Comparative therapeutic effect of NPs1 with trastuzumab plus pertuzumab (T+P), and synergy between NPs1 and lapatinib. **a-c**, Western blot analysis of **(a)** apoptosis related proteins, HER2 total protein, **(b)** inhibition and disaggregation mechanism of HER2 protein dimer and **(c)** inhibition mechanism of proliferation protein in MCF-7/C6 cells treated with NPs1 or combination of T+P for 24 h. Experiments were repeated three times. The concentration of NPs1 used was 50 μM ; The concentration of trastuzumab and pertuzumab used was 15 $\mu\text{g}/\text{mL}$ each. **d,e**, **(d)** The synergistic treatment effect and **(e)** combination index (CI) between NPs1 and lapatinib against MCF-7/C6 cells (In **e**, Fa, fraction affected; CI, combination index; CI value <1 , $=1$, and >1 represent synergy, additive, and antagonism effects, respectively). Data were presented as the mean \pm s.d., $n = 3$ independent experiments. **f-h**, Western blot analysis of **(f)** apoptosis related proteins, HER2 total protein, **(g)** inhibition and disaggregation mechanism of HER2 protein dimer and **(h)** inhibition mechanism of proliferation protein in MCF-7/C6 cells treated with NPs1, lapatinib and NPs1 plus lapatinib for 24 h. Experiments were repeated three times. The concentration of NPs1 and lapatinib used were at 50 μM and 10 μM , respectively.



Supplementary Fig. 37. The *in vitro* and *in vivo* data of control untransformable peptide monomer 5 (TPM5). **a**, Biotinylated scrambled peptide (YFYYGCCVDDMA, blue curve), HER2 peptide ligand (YCDGFYACYMDV, orange curve) and negative control (red curve) incubation with MCF-7/C6 cells were analyzed with flow cytometry. Scrambled peptide sequence possesses very low binding affinity. Experiments were repeated three times. **b**, Mass spectra *via* MALDI-TOF of TPM5. Experiments were repeated three times. **c-e**, (**c**) Self-assembly fluorescence change, $\lambda_{ex} = 380$ nm, (**d**) critical aggregation concentration, (**e**) TEM/zeta

Fig 3g**Fig 5i****Supplementary Fig 35a****Supplementary Fig 36a****Supplementary Fig 36b****Supplementary Fig 36c****Supplementary Fig 36f**

